PHYSICAL REVIEW D **71,** 054016 (2005)

Ground state in a spin-one color superconductor

Andreas Schmitt*

Institut für Theoretische Physik, J. W. Goethe-Universität, D-60054 Frankfurt/Main, Germany

(Received 10 December 2004; revised manuscript received 31 January 2005; published 15 March 2005)

Color superconductors in which quarks of the same flavor form Cooper pairs are investigated. These Cooper pairs carry total spin one. A systematic group-theoretical classification of possible phases in a spin-one color superconductor is presented, revealing parallels and differences to the theory of superfluid ^{3}He. General expressions for the gap parameter, the critical temperature, and the pressure are derived and evaluated for several spin-one phases, with special emphasis on the angular structure of the gap equation. It is shown that the (transverse) color-spin-locked phase is expected to be the ground state.

DOI: 10.1103/PhysRevD.71.054016 PACS numbers: 12.38.Mh, 24.85.+p

I. INTRODUCTION

It is well known that certain metals and alloys exhibit a superconducting phase below a critical temperature T_c. In this phase, electrons in the vicinity of the Fermi surface form Cooper pairs which leads to a gap ϕ in the quasiparticle excitation spectrum [1]. An attractive interaction between the electrons is provided by the exchange of virtual phonons, and the electromagnetic gauge group $U(1)_{\mathrm{em}}$ is spontaneously broken. A similar mechanism occurs in sufficiently cold and dense quark matter [2]. In this case, the attractive color-antitriplet channel is responsible for the formation of quark Cooper pairs. Because of the intrinsic properties of quarks (color, flavor, electric charge), many pairing patterns seem to be theoretically possible. In other words, besides the electromagnetic gauge group, also the color gauge group $SU(3)_c$, the flavor group $SU(N_f)_f$, and the baryon number conservation group $U(1)_B$ may be broken completely or to a certain residual subgroup. In recent years there have been interesting works studying the ground state of cold and dense quark matter, i.e., it has been investigated which color-superconducting phase is favored for certain ranges of the quark chemical potential μ. This question is also of phenomenological interest, since matter in the interior of neutron stars can reach densities up to an order of magnitude larger than the nuclear ground state density while the temperature can be of the order of keV. Therefore, the core of a neutron star can be expected to be a color superconductor and the question arises of which of the color-superconducting phases it consists.

For very large densities, where the quark masses of the u, d, and s quarks can be considered degenerate since they are much smaller than the chemical potential, the ground state is the so-called color-flavor-locked (CFL) phase [3]. In this phase, quarks of all flavors and all colors form Cooper pairs, breaking spontaneously $SU(3)_c \times SU(3)_f \times U(1)_{\mathrm{em}} \times U(1)_B$ to a subgroup $SU(3)_{c+f} \times U(1)_{c+\mathrm{em}}$. At smaller densities the situation is more complicated, because the strange mass cannot be neglected. Furthermore, the conditions of β equilibrium and electric charge neutrality impose restrictive conditions on the system. The simplest solution seems to be a pairing of only u and d quarks [2], the so-called 2SC phase. In this phase, quarks of one color remain unpaired, and the symmetry breaking pattern is $SU(3)_c \times SU(2)_f \times U(1)_{\mathrm{em}} \times U(1)_B \rightarrow SU(2)_c \times SU(2)_f \times U(1)_{c+\mathrm{em}} \times U(1)_{\mathrm{em}+B}$. In both CFL and 2SC phases the Fermi momenta of the quark flavors participating in pairing are assumed to be equal. This is a necessary condition for the conventional BCS pairing mechanism, since in both cases quarks of different flavors form Cooper pairs. However, for moderate densities, this assumption is not valid. Therefore, the ground state is neither the (pure) CFL nor the (pure) 2SC state. Several other possibilities have been discussed. In principle, besides a transition to the normal-conducting state, there are two classes of alternatives, both yielding color-superconducting states. In the first class, the difference in Fermi momenta is nonzero but small enough to still allow for pairing of quarks of different flavors. The second class accounts for cases in which quarks of the same flavor pair.

Let us first mention some options for the first class. First, there might be a phase in which the Cooper pairs carry nonzero total momentum. In this case, the system exhibits a crystalline structure due to a spatially varying energy gap [4]. This kind of superconductivity is called Larkin-Ovchinnikov-Fulde-Ferrell (LOFF) phase and was first discussed in solid-state physics [5], where a difference in the electron Fermi momenta is induced by an external magnetic field. Second, there are studies about the ''gapless'' 2SC [6] and CFL [7] phases. In these phases, at least a part of the quasiparticle excitations are ungapped, although the gap parameter is nonzero. This feature obviously can have enormous physical consequences, for instance for the specific heat and the neutrino emissivity which both affect the cooling of a neutron star with a core in a gapless color-superconducting phase. Other possible phases are derived from the CFL phase and contain

*Present address: Center for Theoretical Physics, MIT, Cambridge, MA 02139, USA.
Electronic address: aschmitt@th.physik.uni-frankfurt.de

kaon and/or eta condensates [8]. Moreover, besides a displacement (LOFF phase), also a deformation of the Fermi surface has been discussed [9].

In this paper, we discuss the possibility of the second class, namely, systems in which quarks of the same flavor form Cooper pairs [2,10–12]. The simplest situation for this kind of color superconductivity is a system of only one quark flavor. More realistic scenarios are two- or three-flavor systems where each quark flavor separately forms Cooper pairs. Another possibility is a system where u and d quarks form a (gapless) 2SC superconductor while the s quarks pair separately.

Since the attractive interaction of quarks is provided in the *antisymmetric* color-antitriplet channel, the spin channel must be symmetric in order to ensure the overall antisymmetry of the Cooper pair wave function. Consequently, Cooper pairs consisting of quarks of the same flavor cannot carry total spin zero but must condense in the spin-one channel, $J = 1$, where $J = L + S$ is the total spin of the Cooper pair, consisting of their angular momentum L and their spin S. This ''two-triplet condensation'' (color and spin triplets) renders the structure of the order parameter a complex 3×3 matrix. This is in contrast to the 2SC case, where, due to condensation in the color-antitriplet, flavor and spin singlet channels, the order parameter is a complex 3-vector. In the CFL case, the order parameter is also a 3×3 matrix, originating from the color and flavor antitriplets.

Another system with this structure of the order parameter is superfluid ^{3}He [13,14]. In this nonrelativistic system, angular momentum L and spin S are separate quantum numbers, both giving rise to a triplet structure of the condensate. In other words, a Cooper pair of ^{3}He atoms carries angular momentum one and spin one. Without external magnetic fields, two phases of superfluid ^{3}He are experimentally known, the A and B phases. The A phase is given by the order parameter structure $\Delta_{ij} = \delta_{i3}(\delta_{j1} + i\delta_{j2})$, where the index i refers to spin and the index j to angular momentum. This order parameter spontaneously breaks $SO(3)_S \times SO(3)_L \times U(1)_N$ to $U(1)_S \times U(1)_{L+N}$, where $SO(3)_S$ and $SO(3)_L$ are the spin and angular momentum groups, respectively, and $U(1)_N$ is the particle number conservation group. The B phase, which covers the largest region of the phase diagram, is given by $\Delta_{ij} = \delta_{ij}$, locking angular momentum with spin. Here, the residual group is $SO(3)_{S+L}$. While the gap function $\phi(\hat{\mathbf{k}})$ is isotropic in the B phase, it is anisotropic in the A phase. The condensation energy (density) Δp of the superfluid states is given by the angular average of the square of the gap [14],

$$\Delta p = \tfrac{1}{2} N(0) \langle \phi^2(\hat{\mathbf{k}}) \rangle_{\hat{\mathbf{k}}}, \tag{1}$$

where $N(0)$ is the density of states at the Fermi surface and $\langle - \rangle_{\hat{\mathbf{k}}} \equiv \int d\Omega_k / 4\pi$. In weak coupling and at zero temperature, the ratio of the condensation energies of the A phase and the B phase is [cf. Eqs. (3.72) and (3.75) of Ref. [14]]

$$\frac{\Delta p_A}{\Delta p_B} \simeq 0.88. \tag{2}$$

Therefore, weak-coupling theory predicts the B phase to be the favored state.

It is the main goal of this paper to determine the favored state in a spin-one color superconductor. The paper is organized as follows: In Sec. II, we discuss possible symmetry breaking patterns in a spin-one color superconductor. In general, the group $G = SU(3)_c \times SU(2)_J \times U(1)_{\mathrm{em}} \times U(1)_B$ is spontaneously broken to a residual group H, where $SU(2)_J$ is the (relativistic) spin group. A systematic list of order parameter matrices Δ and the corresponding residual groups is presented, based on the simple group-theoretical condition that Δ be invariant under transformations of H. Four phases with large residual groups are picked for further investigation in the next sections, namely, the polar, planar, A, and CSL (color-spin-locked) phases.

After establishing the formalism in Sec. III A, Sec. III B is devoted to solving the gap equation for the general case of one or two nonzero (constant or angular-dependent) energy gaps. The results are the gap functions for zero temperature, $T = 0$, at the Fermi surface

$$\phi_r(\hat{\mathbf{k}}) = \sqrt{\lambda_{k,r}}\,\phi_0, \tag{3}$$

where the angular dependence is contained in the quantities $\lambda_{k,r} \equiv \lambda_r(\hat{\mathbf{k}})$. The gap function occurs in the excitation spectrum of the quasiparticles,

$$\epsilon_{k,r} = \sqrt{(k-\mu)^2 + \lambda_{k,r}\phi_0^2}. \tag{4}$$

Let us briefly recall the situation of isotropic gap functions, $\lambda_{k,r} \equiv \lambda_r$. It has been shown that, in this case and with $r = 1, 2$, the gap parameter is given by [11,15–19]

$$\phi_0 = 2\tilde{b} b_0' e^{-d} e^{-\zeta} \mu \exp\!\left(-\frac{\pi}{2\bar{g}}\right), \tag{5}$$

where

$$\bar{g} \equiv \frac{g}{3\sqrt{2}\pi}, \qquad \tilde{b} \equiv 256\pi^4 \left(\frac{2}{N_f g^2}\right)^{5/2}, \qquad b_0' \equiv \exp\!\left(-\frac{\pi^2+4}{8}\right), \tag{6}$$

with the strong coupling constant g. The exponent d is zero in all spin-zero phases and nonzero for $J = 1$. The exponent ζ is defined as

$$\zeta \equiv \ln(\lambda_1^{a_1} \lambda_2^{a_2})^{1/2}, \tag{7}$$

where the numbers a_1 and a_2 have to be determined for each phase separately. They fulfill the condition

$$a_1 + a_2 = 1. \tag{8}$$

The notation $e^{-\zeta}$ instead of $(\lambda_1^{a_1}\lambda_2^{a_2})^{-1/2}$ will turn out to be convenient for the generalization to the case of anisotropic gap functions.

In the case of the 2SC phase, there is only one gapped quasiparticle excitation branch, $a_1 = \lambda_1 = 1$, $a_2 = \lambda_2 = 0$, and hence

$$\phi_0^{\mathrm{2SC}} = 2\tilde{b}b_0'\mu \exp\left(-\frac{\pi}{2\tilde{g}}\right), \tag{9}$$

whereas in the CFL phase, there are two different gaps, $a_1 = 1/3$, $a_2 = 2/3$, $\lambda_1 = 4$, $\lambda_2 = 1$, which leads to $\phi_0^{\mathrm{CFL}} = 2^{-1/3}\phi_0^{\mathrm{2SC}}$.

In Sec. III C, we compute the transition temperature T_c for the transition from the normal-conducting to the superconducting state. As for the gap, this is a generalization of the cases with constant (angular-independent) gaps, for which the transition temperature is given by [19]

$$\frac{T_c}{\phi_0} = \frac{e^\gamma}{\pi} e^\zeta \simeq 0.57 e^\zeta, \tag{10}$$

where $\gamma \simeq 0.577$ is the Euler-Mascheroni constant. It has been one of the main conclusions of Ref. [19] that this expression shows the violation of the well-known BCS relation $T_c/\phi_0 \simeq 0.57$ in the case of a two-gap structure, i.e., $\lambda_{1,2}$, $a_{1,2} \neq 0$. (Also in the case of the gapless 2SC phase, this relation is violated [6].)

As in the case of ^{3}He, one expects the preferred phase to have the largest condensation energy cf. Eq. (1). We specify this statement in Sec. III D with a general derivation of the pressure in an arbitrary color-superconducting phase.

In Sec. IV, we determine the excitation spectrum, the gap functions, the critical temperature, and the pressure for the polar, planar, A, and CSL phases. For each phase we consider three special cases, termed ''longitudinal,'' ''mixed,'' and ''transverse.'' These three cases arise from the following property of spin-one phases: Contrary to a spin-zero color superconductor, where only quarks of the same chirality form Cooper pairs (RR and LL pairs), in a spin-one color superconductor also pairing of quarks with opposite chirality (RL and LR pairs) is possible [11,12,19]. In general, the order parameter contains a linear combination of both kinds of condensates. We focus on the cases of pure RR/LL condensates (longitudinal), a special admixture of RR/LL and RL/LR condensates (mixed), and pure RL/LR condensates (transverse). Consequently, in total 12 phases are studied.

In Sec. V we summarize the results and give an outlook for possible consequences in neutron stars with color-superconducting cores.

Our convention for the metric tensor is $g^{\mu\nu} = \mathrm{diag}\{1, -1, -1, -1\}$. Our units are $\hbar = c = k_B = 1$. Four-vectors are denoted by capital letters, $K \equiv K^\mu = (k_0, \mathbf{k})$, and $k \equiv |\mathbf{k}|$, while $\hat{\mathbf{k}} \equiv \mathbf{k}/k$. We work in the imaginary-time formalism, i.e., $T/V\sum_K \equiv T\sum_n \int d^3\mathbf{k}/(2\pi)^3$, where n labels the Matsubara frequencies $\omega_n \equiv ik_0$. For bosons, $\omega_n = 2n\pi T$, for fermions, $\omega_n = (2n+1)\pi T$.

II. PATTERNS OF SYMMETRY BREAKING

In this section, we discuss possible symmetry breaking patterns in a spin-one color superconductor. In other words, we present a systematic classification of theoretically possible superconducting phases. In the case of a one-flavor, spin-one color superconductor, the relevant original symmetry group of the system is

$$G = G_1 \times G_2 \times G_3, \tag{11}$$

where

$$G_1 = SU(3)_c, \qquad G_2 = SU(2)_J, \qquad G_3 = U(1)_{\mathrm{em}}. \tag{12}$$

Note that the global group $U(1)_B$, accounting for baryon number conservation, has the same generator as the local symmetry group $U(1)_{\mathrm{em}}$. This is not true in a system with $N_f > 1$, when at least two quark flavors differ in their electric charge. In particular, in the CFL phase ($N_f = 3$), this leads to the fact that the system is not an electromagnetic superconductor but a superfluid [the breakdown of $U(1)_B$ gives rise to a Goldstone boson]. For $N_f = 1$, however, these two phenomena are coupled, i.e., a superflow is equivalent to a supercurrent.

The order parameter Δ is an element of a representation of G. In the following, we use the term order parameter somewhat sloppily for the pure matrix structure Δ. For a spin-one color superconductor, the relevant representation of G is the tensor product of the antisymmetric color antitriplet $[\bar{\mathbf{3}}]_c^a$ and the symmetric spin triplet $[\mathbf{3}]_J^s$,

$$\Delta \in [\bar{\mathbf{3}}]_c^a \otimes [\mathbf{3}]_J^s. \tag{13}$$

Therefore, Δ is, as in the case of superfluid ^{3}He, a complex 3×3 matrix. There is no nontrivial contribution from the flavor structure since we consider systems with only one quark flavor. The group G is spontaneously broken down to a residual (proper) subgroup $H \subseteq G$. This means that any transformation $g \in H$ leaves the order parameter invariant,

$$g(\Delta) = \Delta. \tag{14}$$

In the following, we investigate this invariance condition in order to determine all possible order parameters Δ and the corresponding residual groups H. The method we use in this section is motivated by the analogous one for the case of superfluid ^{3}He [14].

First, one has to specify how G acts on the order parameter in Eq. (14). To this end, we write an arbitrary group element $g \in G$ as (in this section, no confusion with the strong coupling constant g is possible)

$$g = (g_1, g_2, g_3), \tag{15}$$

where

$$g_1 = \exp(-ia_m T_m^T), \qquad g_2 = \exp(ib_n J_n), \qquad g_3 = \exp(2ic\mathbf{1}), \tag{16}$$

with real coefficients a_m ($m = 1, \ldots, 8$), b_n ($n = 1, 2, 3$), and c. The Gell-Mann matrices T_m generate the group $SU(3)_c$, and we have taken into account that the color representation is an *antitriplet*. The matrices J_n are the generators of the spin group $SU(2)_J$, $(J_n)_{ij} = -i\epsilon_{nij}$. For the generator of $U(1)$ we choose $2 \times \mathbf{1}$, where $\mathbf{1}$ is the 3×3 unit matrix. The factor 2 accounts for the diquark nature of the order parameter.

Let us now introduce a basis $J_i \otimes \kappa_j$ ($i, j = 1, 2, 3$) for the representation given in Eq. (13). For the basis elements of $[\bar{\mathbf{3}}]_c^a$ we choose the antisymmetric 3×3 matrices J_i, as introduced above as generators of the spin group. The basis of $[\mathbf{3}]_J^s$ is given by the 3-vector κ_j, which will be specified in Sec. IV cf. Eq. (120). Thus, we have to consider the action of G on

$$\mathcal{M}_{\mathbf{k}} \equiv J_i \Delta_{ij} \kappa_j. \tag{17}$$

We have

$$g(\mathcal{M}_{\mathbf{k}}) = g_3 g_1^{ik} J_k \Delta_{ij} g_2^{j\ell} \kappa_\ell. \tag{18}$$

Therefore, the matrix Δ transforms as

$$g(\Delta_{ij}) = g_3 g_1^{ki} \Delta_{k\ell} g_2^{\ell j}. \tag{19}$$

Then, using Eqs. (16), the infinitesimal transformations of Δ by G are given by

$$g(\Delta) \simeq \Delta - a_m T_m \Delta + b_n \Delta J_n + 2c\Delta, \tag{20}$$

where $T_m\Delta$ as well as ΔJ_n are matrix products. The invariance condition for the order parameter (14) is thus equivalent to

$$-a_m T_m \Delta + b_n \Delta J_n + 2c\Delta = 0. \tag{21}$$

This matrix equation can be written as a system of nine equations for the nine complex entries $\Delta_{11}, \ldots, \Delta_{33}$ of the matrix Δ. In principle, one can find all possible symmetry breaking patterns and corresponding order parameters by setting the determinant of the coefficient matrix to zero. Then, each possibility to render the determinant zero yields a set of conditions for the coefficients a_m, b_n, c, and it can be checked if these conditions correspond to a residual subgroup H. But since this is much too complicated, we proceed via investigating possible subgroups explicitly. In the following, we focus only on the continuous subgroups of G.

Let us start with subgroups H that contain the smallest possible continuous group, $U(1)$, i.e.,

$$H = U(1) \times H', \tag{22}$$

where H' is a direct product of Lie groups. The residual $U(1)$ must be generated by a 3×3 matrix U which is a linear combination of the generators of G, i.e., in general,

$$U = a_m T_m + b_n J_n + 2c\mathbf{1}. \tag{23}$$

Let us restrict ourselves to linear combinations that involve one generator of each group G_1, G_2, G_3, for instance

$$U = a_8 T_8 + b_3 J_3 + 2c\mathbf{1}. \tag{24}$$

With Eq. (24), the invariance condition

$$e^{iU}(\Delta) = \Delta \tag{25}$$

results in a system of nine equations, which can be discussed explicitly. This is done in Appendix A. We find ten different order parameters, eight of them depending on two or more parameters $\Delta_1, \Delta_2, \ldots$, which physically corresponds to more than one gap function. With the normalization

$$\mathrm{Tr}(\Delta\Delta^\dagger) = 1, \tag{26}$$

the calculation in Appendix A yields also two matrices Δ that do not depend on any free parameter (which corresponds to only one gap function). In analogy to ^{3}He, let us call the phases defined by this kind of order parameter *inert* [14]. All experimentally known states of superfluid ^{3}He belong to this class of order parameters. Mathematically speaking, these matrices play a special role due to a theorem (''Michel's Theorem'') [14,20], which ensures that these order parameters correspond to a stationary point of any G-invariant functional of Δ (for instance the effective potential). This is the reason why we also focus on these order parameters in the explicit calculations of the physical properties, see Sec. IV.

One order parameter, found with the ansatz (24) and corresponding to an inert phase, is

$$\Delta = \begin{pmatrix} 0 & 0 & 0 \\ 0 & 0 & 0 \\ 0 & 0 & 1 \end{pmatrix}, \tag{27}$$

defining the *polar phase*. It has its analogue in ^{3}He [14], where the order parameter matrix is identical. For the case of a color superconductor, certain aspects of the polar phase have already been discussed in Refs. [12,19,21,22]. For the corresponding residual group H see Fig. 1, where we list all order parameters. More details, especially the explicit forms of the generators of H, are given in Appendix A. The second-order parameter giving rise to an inert phase is

$$\Delta = \frac{1}{\sqrt{2}} \begin{pmatrix} 0 & 0 & 0 \\ 0 & 0 & 0 \\ 1 & i & 0 \end{pmatrix}. \tag{28}$$

This order parameter leads to the *A phase* [12,14].

In order to find all possible (inert) order parameters, it is necessary to consider at least one more combination for the residual $U(1)$ in Eq. (22), namely

$$U = a_2 T_2 + b_3 J_3 + 2c\mathbf{1}. \tag{29}$$

phase	$SU(3)_c$ x $SU(2)_J$ x $U(1)_{em}$ broken to	order parameter
polar	$SU(2)$ x $U(1)$ x $U(1)$	$\begin{pmatrix} 0 & 0 & 0 \\ 0 & 0 & 0 \\ 0 & 0 & 1 \end{pmatrix}$
planar	$U(1)$ x $U(1)$	$\begin{pmatrix} 1 & 0 & 0 \\ 0 & 1 & 0 \\ 0 & 0 & 0 \end{pmatrix}$
A	$SU(2)$ x $U(1)$ x $U(1)$	$\begin{pmatrix} 0 & 0 & 0 \\ 0 & 0 & 0 \\ 1 & i & 0 \end{pmatrix}$
CSL	$SU(2)$	$\begin{pmatrix} 1 & 0 & 0 \\ 0 & 1 & 0 \\ 0 & 0 & 1 \end{pmatrix}$
P_1	$SU(2)$ x $U(1)$	$\begin{pmatrix} 0 & 0 & 0 \\ 0 & 0 & 0 \\ \Delta_1 & \Delta_2 & \Delta_3 \end{pmatrix}$
P_2	$U(1)$ x $U(1)$	$\begin{pmatrix} 0 & 0 & \Delta_1 \\ 0 & 0 & \Delta_2 \\ 0 & 0 & 0 \end{pmatrix}$
P_3	$U(1)$ x $U(1)$	$\begin{pmatrix} \Delta_1 & i\Delta_1 & 0 \\ \Delta_2 & i\Delta_2 & 0 \\ 0 & 0 & 0 \end{pmatrix}$
P_4	$U(1)$	$\begin{pmatrix} \Delta_1 & \Delta_2 & \Delta_3 \\ \Delta_4 & \Delta_5 & \Delta_6 \\ 0 & 0 & 0 \end{pmatrix}$
P_5	$U(1)$	$\begin{pmatrix} \Delta_1 & i\Delta_1 & 0 \\ \Delta_2 & i\Delta_2 & 0 \\ \Delta_3 & i\Delta_3 & 0 \end{pmatrix}$
P_6	$U(1)$	$\begin{pmatrix} 0 & 0 & \Delta_1 \\ 0 & 0 & \Delta_2 \\ 0 & 0 & \Delta_3 \end{pmatrix}$
P_7, P_8	$U(1)$	$\begin{pmatrix} \Delta_1 & i\Delta_1 & 0 \\ \Delta_2 & i\Delta_2 & 0 \\ 0 & 0 & \Delta_3 \end{pmatrix}$, $\begin{pmatrix} 0 & 0 & \Delta_1 \\ 0 & 0 & \Delta_2 \\ \Delta_3 & i\Delta_3 & 0 \end{pmatrix}$

FIG. 1. Symmetry breaking patterns and order parameters for a spin-one color superconductor. The original symmetry group (first line) is given by the color gauge group $SU(3)_c$ (blank background), the spin group $SU(2)_J$ (gray background), and the electromagnetic gauge group $U(1)_{\mathrm{em}}$ (hatched background). The backgrounds of the residual groups illustrate the symmetry breaking pattern. For instance, the blank $SU(2)$ occurring in the residual group of the polar phase is generated solely by generators of the original $SU(3)_c$ while the blank/hatched $U(1)$ in the same line is generated by a linear combination of the generators of the original $SU(2)_J$ and $U(1)_{\mathrm{em}}$ groups. For the explicit expression of these generators, see text.

The reason why T_2 plays a special role is that we used the generator J_3 of the spin group, which is proportional to T_2. Consequently, we expect to find additional residual groups that connect the color group with the spin group [meaning a residual $U(1)$ generated by a combination of a color and a spin generator]. The calculations with this generator are completely analogous to the ones with the ansatz (24). Therefore, we present the result without elaborating on

the details. The ansatz (29) yields one inert order parameter that is different from the above ones, namely

$$\Delta = \frac{1}{\sqrt{2}} \begin{pmatrix} 1 & 0 & 0 \\ 0 & 1 & 0 \\ 0 & 0 & 0 \end{pmatrix}. \tag{30}$$

This order parameter corresponds to the *planar phase* [12,14]. The residual group is $H = U(1) \times U(1)$, with generators

$$U = 2T_2 + J_3, \qquad V = T_8 + \frac{1}{4\sqrt{3}}\mathbf{1}. \tag{31}$$

Let us now turn to possible groups H that do not contain any $U(1)$ but solely consist of higher-dimensional Lie groups, say

$$H = SU(2) \times H'. \tag{32}$$

Let U_1, U_2, U_3 be the generators of the residual $SU(2)$. They are linear combinations of the generators of G,

$$U_i = a^i_m T_m + b^i_n J_n + 2c^i \mathbf{1}, \qquad i = 1, 2, 3. \tag{33}$$

Since they must fulfill the $SU(2)$ commutation relations,

$$[J_i, J_j] = i\epsilon_{ijk} J_k, \qquad i, j, k \leq 3, \tag{34}$$

they must not contain the generator of $G_3 = U(1)$, the unit matrix, i.e., $c^1 = c^2 = c^3 = 0$. Therefore, there are three possibilities. First, each U_i is a combination of color and spin generators. Second and third, each U_i is composed solely of color or spin generators, respectively. The simplest options to realize these cases are

$$U_i = T'_i + J_i, \tag{35a}$$
$$U_i = T'_i, \tag{35b}$$
$$U_i = J_i, \tag{35c}$$

where (T'_1, T'_2, T'_3) is either given by (T_1, T_2, T_3) or $(2T_7, -2T_5, 2T_2)$, which both fulfill the required commutation relations. Using the options (35a)–(35c), let us first show that H' in Eq. (32) cannot be a second $SU(2)$. To this end, assume that $H' = SU(2)$ with generators V_1, V_2, V_3, which have the same form as the generators U_i in Eqs. (35). Then, since the Lie algebra of H is a direct sum of the constituent Lie algebras, we have to require

$$[U_i, V_j] = 0. \tag{36}$$

This condition reduces all options to one, namely

$$U_i = T'_i, \qquad V_i = J_i \tag{37}$$

(or vice versa). However, now the invariance equation for the order parameter yields

$$\Delta J_i = 0, \tag{38}$$

for all $i = 1, 2, 3$, which does not allow for a nonzero order parameter Δ. Therefore, $H' = SU(2)$ is forbidden. Since the cases with $H' = U(1)$ and $H' = U(1) \times U(1)$ were already covered in the above discussion, the only possibility that is left is $H' = \mathbf{1}$ and thus $H = SU(2)$.

The generators in Eq. (35c) can immediately be excluded since they also lead to Eq. (38). The same argument excludes case (35b) with $(T'_1, T'_2, T'_3) = (2T_7, -2T_5, 2T_2)$. Case (35b) with $(T'_1, T'_2, T'_3) = (T_1, T_2, T_3)$ leads to two order parameters already considered above, namely, the polar phase, Eq. (27), and the A phase, Eq. (28). In case (35a), only $(T'_1, T'_2, T'_3) = (2T_7, -2T_5, 2T_2)$ is possible. With

$$U_i \Delta = -T'_i \Delta + \Delta J_i = 0, \tag{39}$$

one finds

$$\Delta = \frac{1}{\sqrt{3}} \begin{pmatrix} 1 & 0 & 0 \\ 0 & 1 & 0 \\ 0 & 0 & 1 \end{pmatrix}. \tag{40}$$

Indeed, it can be checked with Eq. (21) that this order parameter leads to

$$a_1 = a_3 = a_4 = a_6 = a_8 = c = 0, \qquad a_2 = 2b_3, \qquad a_5 = -2b_2, \qquad a_7 = 2b_1, \tag{41}$$

which corresponds to $H = SU(2)$, consisting of joint rotations in color and spin space. This is the *CSL phase*, discussed for a spin-one color superconductor in Refs. [2,12,19,21,22]. It is the analogue of the B phase in superfluid ^{3}He.

Finally, we give an argument why an even larger subgroup, i.e., an $SU(3)$, cannot occur in the residual group H. Assume that there are eight generators $W_1, \ldots, W_8$ of this $SU(3)$. Then, as for the $SU(2)$ subgroup above, there can be no contribution to $W_1, \ldots, W_8$ from the G_3 generator due to the $SU(3)$ commutation relations for the generators,

$$[W_i, W_j] = i f_{ijk} W_k, \qquad i, j, k \leq 8, \tag{42}$$

where f_{ijk} are the $SU(3)$ structure constants. Also, $W_i = T_i$ is excluded because in this case the invariance condition yields $T_8 \Delta = 0$ and thus $\Delta = 0$. Therefore, at least one of the spin generators has to be included. For instance, choose $W_8 = T_8 + b_3 J_3$. Then, from the commutation relation $[W_4, W_5] \sim W_8$ we conclude that also J_1 and J_2 must be included via $W_4 = T_4 + b_1 J_1$ and $W_5 = T_5 + b_2 J_2$. But now the three equations $W_4 \Delta = W_5 \Delta = W_8 \Delta = 0$ lead to $\Delta = 0$. Therefore, we conclude that there is no residual group H that contains an $SU(3)$. For a more rigorous proof

one has to take into account more complicated linear combinations of the original generators.

In Fig. 1, we summarize our results in a list of all superconducting phases that we have found in the above discussion. It should be mentioned that this list is not complete, since for the generators of the residual $U(1)$'s we have restricted ourselves to two special forms given in Eqs. (24) and (29). Therefore, there are certainly more (at least noninert) order parameters that lead to an allowed symmetry breaking. The inert states are listed in the first four lines. Each of these four states has its analogue in superfluid ^{3}He. Note that the A_1 phase, which is experimentally observed in ^{3}He in the presence of an external magnetic field, does not lead to an allowed symmetry breaking in the case of a spin-one color superconductor [12]. To see this, one inserts the order parameter of the A_1 phase,

$$\Delta = \frac{1}{2}\begin{pmatrix} 1 & i & 0 \\ -i & 1 & 0 \\ 0 & 0 & 0 \end{pmatrix}, \tag{43}$$

into Eq. (21). One obtains

$$a_1 = a_3 = b_1 = b_2 = 0, \qquad a_4 = a_7, \qquad a_5 = a_6, \qquad \frac{1}{2}a_2 + \frac{1}{2\sqrt{3}}a_8 - b_3 - 2c = 0. \tag{44}$$

These seven conditions suggest that $\dim H = 12 - 7 = 5$ and thus $H = SU(2) \times U(1) \times U(1)$. However, there is no possibility to construct three generators from the above conditions that fulfill the $SU(2)$ commutation relations. For instance, assume that two of these generators are given by $U_1 = T_4 + T_7$ and $U_2 = T_5 + T_6$. Then, with Eq. (42), $[U_1, U_2] \sim T_3$. But since $a_3 = 0$, the third generator U_3 cannot be proportional to T_3. Consequently, there is no A_1 phase in a spin-one color superconductor.

Below the four inert states we list the eight noninert states which have been found in Appendix A and which we term $P_1, \ldots, P_8$. Note that one of these noninert phases, P_1, has a larger residual symmetry group than the planar and CSL phases.

There are several properties of the spin-one phases which can easily be read off from Fig. 1. First, consider the spin group $SU(2)_J$. This symmetry accounts for the rotational symmetry in real space of the normal-conducting phase [in the case of the spin-one representation, one can equivalently consider $SO(3)_J$ instead of $SU(2)_J$]. The list shows that spatial symmetry is broken in each case. For instance, in the polar phase, $SU(2)_J$ is broken to its subgroup $U(1)_J$. Therefore, the superconducting phase is invariant under rotations around one fixed axis in real space. In most of the other cases, the breaking of the spatial rotation symmetry is more subtle: For instance in the planar phase, the superconducting state is invariant under a special joint rotation in color and real space. The most interesting breakdown of spatial symmetries is present in the CSL phase. Here, any rotation in real space leaves the system invariant as long as one simultaneously performs the same rotation in fundamental color space which is spanned by the three directions red, green, and blue.

Next, let us read off some properties concerning the color symmetry. It is obvious that in none of the cases the full color symmetry is preserved. In this sense, it is justified to call each phase a color superconductor. In three of the cases, there is a residual color subgroup $SU(2)$, namely, in the polar phase, the A phase, and the P_1 phase. Mathematically speaking, this residual group originates from the fact that the order parameter has only nonzero elements in its third row. Therefore, the third direction in fundamental color space is preferred. Physically, this means that the Cooper pairs carry color charge antiblue, or, in other words, only red and green quarks form Cooper pairs. Of course, the choice of the antiblue direction is convention; more generally speaking, quarks of one color remain unpaired. Remember that this is also true for the 2SC phase.

A spontaneously broken gauge symmetry gives rise to massive gauge bosons. In the case of a color superconductor, these masses are the magnetic screening masses of the gluons. Therefore, in the cases where there is a residual color subgroup $SU(2)$, we expect a Meissner effect for five of the eight gluons. Three of the gluons, however, namely, those corresponding to the generators T_1, T_2, T_3, do not attain a Meissner mass. This is also obvious from the fact that these gluons do not see the (anti)blue color charge which is carried by the Cooper pairs. Also with respect to the breakdown of the color symmetry, the CSL phase is exceptional. Although there is a residual $SU(2)$, where three of the color generators are involved, we expect all eight gluons to attain a Meissner mass. To this end, note that this residual $SU(2)$ is a global symmetry and therefore all dimensions of the gauge group have to be considered as broken. This is analogous to the CFL phase, which also exhibits a color Meissner effect for all eight gluons [23]. For a more detailed and quantitative discussion of the color Meissner effect, see Ref. [22].

In order to discuss the question whether the color superconductors in Fig. 1 are also electromagnetic superconductors, one has to consider the hatched backgrounds in the residual groups. From ordinary superconductors, we know that $U(1)_{\mathrm{em}}$ is spontaneously broken below the critical temperature. Therefore, a simple conclusion is that all states in the list without a hatched background occurring in the residual group are electromagnetic superconductors. Obviously, this is the case for the CSL phase and for one of the noninert states, namely, the P_6 phase. The electromagnetic Meissner effect in the CSL and polar phases has been discussed in detail in Refs. [21,22]. In particular, it has been shown that also the polar phase exhibits an electromagnetic Meissner effect in the case of a many-flavor system, where at least two of the quark flavors have nonequal electric charges.

III. GAPS, TRANSITION TEMPERATURE, AND PRESSURE

In this section, we derive general expressions for the gaps (Sec. III B), the transition temperature (Sec. III C), and the pressure (Sec. III D), valid for all color-superconducting phases we consider. In Sec. IV we evaluate these expressions for several spin-one color superconductors.

A. Notations and definitions

The starting point is the effective action Γ, which yields the gap equation as well as the effective potential $V_{\rm eff} \equiv -\frac{T}{V}\Gamma$ and the pressure p, which is the negative of the effective potential at its stationary point, $p = -V_{\rm eff}$.

The effective action Γ can be derived from the QCD partition function using the Cornwall-Jackiw-Tomboulis (CJT) formalism [24]. The resulting functional can be written as [25–27]

$$\begin{aligned}\Gamma[D_G, D_F] = &-\tfrac{1}{2}\mathrm{Tr}\ln D_G^{-1} - \tfrac{1}{2}\mathrm{Tr}(\Delta_0^{-1}D_G - 1)\\ &+ \tfrac{1}{2}\mathrm{Tr}\ln D_F^{-1} + \tfrac{1}{2}\mathrm{Tr}(S_0^{-1}D_F - 1)\\ &+ \Gamma_2[D_G, D_F].\end{aligned} \tag{45}$$

Here, D_G (Δ_0) and D_F (S_0) are the full (tree-level) gluon and fermion propagators, respectively. All propagators are defined in Nambu-Gor'kov space. We account for the doubling of degrees of freedom in this basis by introducing the factor $1/2$. The traces run over Nambu-Gor'kov, Dirac, flavor, color, and momentum space, and $\Gamma_2[D_G, D_F]$ denotes the sum of all two-particle irreducible diagrams. In the following, we will consider the two-loop approximation of this sum which, for the fermionic degrees of freedom, is equivalent to taking into account only one diagram (the "sunset" diagram [27]). The stationarity conditions for $\Gamma[D_G, D_F]$ yield Dyson-Schwinger equations for the inverse gluon and fermion propagators,

$$\Delta^{-1} = \Delta_0^{-1} + \Pi, \tag{46a}$$

$$S^{-1} = S_0^{-1} + \Sigma. \tag{46b}$$

Here, the pair of propagators (Δ, S) is the stationary point of the effective potential and we defined the gluon and fermion self-energies as

$$\begin{aligned}\Pi &\equiv -2\frac{\delta\Gamma_2}{\delta D_G}\bigg|_{(D_G,D_F)=(\Delta,S)},\\ \Sigma &\equiv 2\frac{\delta\Gamma_2}{\delta D_F}\bigg|_{(D_G,D_F)=(\Delta,S)}.\end{aligned} \tag{47}$$

The free inverse fermion propagator is

$$S_0^{-1} = \begin{pmatrix}[G_0^+]^{-1} & 0\\ 0 & [G_0^-]^{-1}\end{pmatrix}, \tag{48}$$

where $[G_0^+]^{-1}$ and $[G_0^-]^{-1}$ are the free inverse propagators for massless quarks and massless charge-conjugate quarks in the presence of a chemical potential μ,

$$[G_0^\pm]^{-1} = \gamma^\mu K_\mu \pm \mu\gamma_0. \tag{49}$$

In order to find the full propagators, one has to solve the Dyson-Schwinger equations, Eq. (46a), self-consistently. To this end, we denote the entries of the fermion self-energy in Nambu-Gor'kov space by

$$\Sigma \equiv \begin{pmatrix}\Sigma^+ & \Phi^-\\ \Phi^+ & \Sigma^-\end{pmatrix}, \tag{50}$$

and invert Eq. (46b) formally [28], which yields the full quark propagator in the form

$$S = \begin{pmatrix}G^+ & \Xi^-\\ \Xi^+ & G^-\end{pmatrix}, \tag{51}$$

where the fermion propagators for quasiparticles and charge-conjugate quasiparticles are

$$G^\pm = \{[G_0^\pm]^{-1} + \Sigma^\pm - \Phi^\mp([G_0^\mp]^{-1} + \Sigma^\mp)^{-1}\Phi^\pm\}^{-1}, \tag{52}$$

and the so-called anomalous propagators, typically nonzero for a superconducting system, are given by

$$\Xi^\pm = -([G_0^\mp]^{-1} + \Sigma^\mp)^{-1}\Phi^\pm G^\pm. \tag{53}$$

In the two-loop approximation of Γ_2, the quark self-energy $\Sigma(K)$ in momentum space is

$$\Sigma(K) = -g^2\frac{T}{V}\sum_Q \Gamma_a^\mu S(Q)\Gamma_b^\nu \Delta_{\mu\nu}^{ab}(K-Q), \tag{54}$$

where

$$\Gamma_a^\mu \equiv \begin{pmatrix}\gamma^\mu T_a & 0\\ 0 & -\gamma^\mu T_a^T\end{pmatrix}, \tag{55}$$

with the Gell-Mann matrices T_a, $a = 1, \ldots, 8$. Because of the Nambu-Gor'kov structure, Eq. (54) is actually a set of four equations. With Eqs. (50) and (51), the off-diagonal (21)-component leads to the gap equation

$$\Phi^+(K) = g^2\frac{T}{V}\sum_Q \gamma^\mu T_a^T \Xi^+(Q)\gamma^\nu T_b \Delta_{\mu\nu}^{ab}(K-Q). \tag{56}$$

The quantities $\Phi^\pm(K)$ are matrices in flavor, color, and Dirac space and functions of the quark four-momentum K. Both quantities are related via

$$\Phi^- = \gamma_0[\Phi^+]^\dagger\gamma_0. \tag{57}$$

Following Ref. [19], we term the matrix $\Phi^+(K)$ *gap matrix* and use, for condensation in the even-parity channel and in the ultrarelativistic limit, the ansatz

$$\Phi^+(K) = \sum_{e=\pm}\phi_e(K)\mathcal{M}_{\mathbf{k}}\Lambda_{\mathbf{k}}^e. \tag{58}$$

The Dirac matrices $\Lambda_{\mathbf{k}}^e \equiv (1 + e\gamma_0\boldsymbol{\gamma}\cdot\hat{\mathbf{k}})/2$, where $e = \pm$, are projectors onto positive and negative energy states, and $\phi_e(K)$ is the gap function. The quantity $\mathcal{M}_{\mathbf{k}}$ is a

matrix in color, flavor, and Dirac space. It is defined by the order parameter and thus determines the color-superconducting phase. For the explicit form of $\mathcal{M}_{\mathbf{k}}$ in the case of a spin-one color superconductor, see Eq. (120). We can always choose $\mathcal{M}_{\mathbf{k}}$ such that it commutes with the energy projectors,

$$[\mathcal{M}_{\mathbf{k}}, \Lambda^e_{\mathbf{k}}] = 0. \tag{59}$$

The diagonal elements of the quark self-energy can be approximated as [17,18]

$$\Sigma^+ = \Sigma^- \simeq \gamma_0 \bar{g}^2 k_0 \ln\frac{M^2}{k_0^2}, \tag{60}$$

where $M^2 = (3\pi/4)m_g^2$; the zero-temperature gluon mass parameter (squared) is $m_g^2 = N_f g^2 \mu^2/(6\pi^2)$.

Using Eqs. (52), (58), and (60), we find for the fermion propagators

$$G^{\pm} = ([G_0^{\mp}]^{-1} + \Sigma^{\mp})\sum_{e,r} \mathcal{P}^{\pm}_{\mathbf{k},r}\Lambda^{\mp e}_{\mathbf{k}} \frac{1}{[k_0/Z(k_0)]^2 - (\epsilon^e_{\mathbf{k},r})^2}, \tag{61}$$

where

$$Z(k_0) \equiv \left(1 + \bar{g}^2 \ln\frac{M^2}{k_0^2}\right)^{-1} \tag{62}$$

is the wave function renormalization factor introduced in Ref. [28]. In Eq. (61) we introduced two sets of projectors, $\mathcal{P}^+_{\mathbf{k},r}$ and $\mathcal{P}^-_{\mathbf{k},r}$; they project onto the eigenspaces of the matrices

$$L^+_{\mathbf{k}} \equiv \gamma_0 \mathcal{M}^\dagger_{\mathbf{k}} \mathcal{M}_{\mathbf{k}} \gamma_0 \quad \text{and} \quad L^-_{\mathbf{k}} \equiv \mathcal{M}_{\mathbf{k}} \mathcal{M}^\dagger_{\mathbf{k}}, \tag{63}$$

respectively, i.e., if the number of different eigenvalues $\lambda_{k,r}$ is n, the projectors are [29]

$$\mathcal{P}^{\pm}_{\mathbf{k},r} = \prod_{s\neq r}^{n} \frac{L^{\pm}_{\mathbf{k}} - \lambda_{k,s}}{\lambda_{k,r} - \lambda_{k,s}}. \tag{64}$$

In the case of spin-zero color superconductors (2SC and CFL), $L^+_{\mathbf{k}}$ and $L^-_{\mathbf{k}}$ are identical. But this is not true for all spin-one phases as we shall see in Sec. IV. However, in all phases we consider, $L^+_{\mathbf{k}}$ and $L^-_{\mathbf{k}}$ have the same spectrum. Consequently,

$$L^{\pm}_{\mathbf{k}} = \sum_r \lambda_{k,r}\mathcal{P}^{\pm}_{\mathbf{k},r}. \tag{65}$$

We denote the degeneracy of the eigenvalue $\lambda_{k,r}$ by

$$n_r \equiv \mathrm{Tr}[\mathcal{P}^{\pm}_{\mathbf{k},r}]. \tag{66}$$

In general, the eigenvalues $\lambda_{k,r}$ depend on the direction of the quark momentum $\hat{\mathbf{k}}$ (they do not depend on the modulus k). They enter the quasiparticle excitation energies introduced in Eq. (61),

$$\epsilon^e_{\mathbf{k},r} \equiv \sqrt{(ek - \mu)^2 + \lambda_{k,r}|\phi_e|^2}. \tag{67}$$

Consequently, the spectrum of the matrices $L^{\pm}_{\mathbf{k}}$ determines the structure of the quasiparticle excitations. In all phases we consider, there are at most three different eigenvalues, and at most two different *nonzero* eigenvalues $\lambda_{k,r}$. A zero eigenvalue corresponds to an ungapped excitation branch. This is for instance the case in the 2SC phase, where the ungapped blue quarks give rise to a zero eigenvalue $\lambda_2 = 0$, while $\lambda_1 = 1$. Two different nonzero eigenvalues correspond to two excitation branches with different gaps, well known from the CFL phase, where there is a quasiparticle singlet with gap 2ϕ ($\lambda_1 = 4$ with degeneracy 1) and a quasiparticle octet with gap ϕ ($\lambda_2 = 1$ with degeneracy 8). In the case of the spin-one phases, the eigenvalues carry the potential angular dependence of the energy gap. In the following we assume that there is no additional angular dependence in the functions ϕ_e. Moreover, since we neglect the antiparticle gap, $\phi_- \simeq 0$, we may denote the particle gap by $\phi \equiv \phi_+$. We assume this function to be real, $|\phi|^2 = \phi^2$, and denote the value of this function at the Fermi surface by ϕ_0. With these assumptions and notations we can define the root-mean square (quadratic mean) of the function $\sqrt{\lambda_{k,r}}\phi_0$ as

$$\overline{\phi}_r \equiv \sqrt{\langle\lambda_{k,r}\rangle_{\hat{\mathbf{k}}}}\,\phi_0. \tag{68}$$

Furthermore, for the following it is convenient to define the normalized eigenvalue

$$\hat{\lambda}_{k,r} \equiv \frac{\lambda_{k,r}}{\langle\lambda_{k,r}\rangle_{\hat{\mathbf{k}}}}. \tag{69}$$

We make use of these definitions in the final results cf. Eqs. (98), (103), and (118).

Finally, we determine the anomalous propagator Ξ^+. Inserting the expression for the propagator G^+, Eq. (61), into the definition (53) and using the form of the gap matrix Φ^+ given in Eq. (58), we obtain

$$\Xi^+(K) = -\sum_{e,r} \gamma_0 \mathcal{M}_{\mathbf{k}} \gamma_0 \mathcal{P}^+_{\mathbf{k},r}\Lambda^{-e}_{\mathbf{k}} \frac{\phi_e(K)}{[k_0/Z(k_0)]^2 - (\epsilon^e_{\mathbf{k},r})^2}. \tag{70}$$

B. Solution of the gap equation for an anisotropic gap

In this section, we solve the gap equation for the general case of an anisotropic gap function. Formally, with the definitions of the previous section, this means that we allow for angular-dependent eigenvalues $\lambda_{k,r}$. Starting from the gap equation (56) for the gap matrix $\Phi^+(K)$, we obtain a gap equation for the function $\phi_e(K)$ by inserting Eqs. (58) and (70) into Eq. (56), multiplying both sides with $\mathcal{M}^\dagger_{\mathbf{k}}\Lambda^e_{\mathbf{k}}$, and taking the trace over color, flavor, and Dirac space. Moreover, we use the gluon propagator in the hard-dense-loop approximation, which is permissible to subleading order [30]. We denote quasiparticle energies by $\epsilon_{\mathbf{q},s} \equiv \epsilon^+_{\mathbf{q},s}$, because, due to $\phi^- \simeq 0$, the *quasiantipar-*

ticle energies do not occur in the gap equation. Since the effect of the wave function renormalization factor $Z(k_0)$ for the gap is known [17,18] and does not affect the angular structure of the equation, we omit it for simplicity. The resulting factor b_0', see Eq. (6) can easily be reinserted into the final result. We arrive at

$$\phi(K) = g^2 \frac{T}{V} \sum_Q \sum_s \frac{\phi(Q)}{q_0^2 - \epsilon_{\mathbf{q},s}^2} \Delta^{\mu\nu}(K-Q) \mathcal{T}^s_{\mu\nu}(\mathbf{k},\mathbf{q}), \tag{71}$$

where, following Ref. [19], we have defined

$$\mathcal{T}^{\ s}_{\mu\nu}(\mathbf{k},\mathbf{q}) \equiv -\frac{\mathrm{Tr}[\gamma_\mu T_a^T \gamma_0 \mathcal{M}_\mathbf{q} \gamma_0 \mathcal{P}^+_{\mathbf{q},s} \Lambda^-_\mathbf{q} \gamma_\nu T_a \mathcal{M}^\dagger_\mathbf{k} \Lambda^+_\mathbf{k}]}{\mathrm{Tr}[\mathcal{M}_\mathbf{k} \mathcal{M}^\dagger_\mathbf{k} \Lambda^+_\mathbf{k}]}. \tag{72}$$

With $P \equiv K - Q$, the gluon propagator in pure Coulomb gauge is given by

$$\begin{aligned} \Delta^{00}(P) &= \Delta_\ell(P), \qquad \Delta^{0i}(P) = 0, \\ \Delta^{ij}(P) &= (\delta^{ij} - \hat{p}^i \hat{p}^j) \Delta_t(P). \end{aligned} \tag{73}$$

For the definition of the longitudinal and transverse gluon propagators $\Delta_{\ell,t}$ see for instance Ref. [11]. With the (negative) transverse projection of the tensor $\mathcal{T}^s_{\mu\nu}(\mathbf{k},\mathbf{q})$,

$$\mathcal{T}^{\ s}_t(\mathbf{k},\mathbf{q}) \equiv -(\delta^{ij} - \hat{p}^i \hat{p}^j) \mathcal{T}^s_{ij}(\mathbf{k},\mathbf{q}), \tag{74}$$

we obtain after performing the Matsubara sum (for details see Ref. [11]), and after taking the thermodynamic limit, $V \to \infty$,

$$\begin{aligned} \phi_{k,r} = \frac{g^2}{4} \int \frac{d^3q}{(2\pi)^3} \sum_s \frac{\phi_{q,s}}{\epsilon_{\mathbf{q},s}} \tanh\!\left(\frac{\epsilon_{\mathbf{q},s}}{2T}\right) \\ \times [F_\ell(p) \mathcal{T}^s_{00}(\mathbf{k},\mathbf{q}) + F_t(p, \epsilon_{\mathbf{q},s}, \epsilon_{\mathbf{k},r}) \mathcal{T}^s_t(\mathbf{k},\mathbf{q})], \end{aligned} \tag{75}$$

where

$$F_\ell(p) \equiv \frac{2}{p^2 + 3m_g^2} \tag{76}$$

arises from static electric gluons, while

$$\begin{aligned} F_t(p, \epsilon_{\mathbf{q},s}, \epsilon_{\mathbf{k},r}) \equiv \frac{2}{p^2} \Theta(p-M) + \Theta(M-p) \\ \times \left[\frac{p^4}{p^6 + M^4(\epsilon_{\mathbf{q},s} + \epsilon_{\mathbf{k},r})^2} \right. \\ \left. + \frac{p^4}{p^6 + M^4(\epsilon_{\mathbf{q},s} - \epsilon_{\mathbf{k},r})^2} \right] \end{aligned} \tag{77}$$

originates from nonstatic and almost static magnetic gluons. In Eq. (75) we have abbreviated $\phi_{k,r} \equiv \phi(\epsilon_{\mathbf{k},r}, \mathbf{k})$ and $\phi_{q,s} \equiv \phi(\epsilon_{\mathbf{q},s}, \mathbf{q})$. At this point, the angular integral $d\Omega_q$ on the right-hand side of Eq. (75) seems to be too complicated, since, besides the square of the gluon 3-momentum $p^2 = k^2 + q^2 - 2\mathbf{q}\cdot\mathbf{k}$ and the functions $\mathcal{T}^s_{00}$, $\mathcal{T}^s_t$, also the excitation energies $\epsilon_{\mathbf{q},s}$ depend on the direction of $\mathbf{q}$. The solution to this problem is to multiply both sides of the equation with

$$\ell_k \equiv \mathrm{Tr}[\mathcal{M}_\mathbf{k} \mathcal{M}^\dagger_\mathbf{k} \Lambda^+_\mathbf{k}] = \frac{1}{2} \sum_r n_r \lambda_{k,r}, \tag{78}$$

and take the angular average over $\hat{\mathbf{k}}$ of the whole equation. The right-hand side of Eq. (78) is obtained with the help of Eqs. (63), (65), and (66), and the following identities:

$$\tfrac{1}{2} \mathrm{Tr}[\mathcal{P}^+_{\mathbf{k},r}] = \mathrm{Tr}[\mathcal{P}^+_{\mathbf{k},r} \Lambda^e_\mathbf{k}] = \mathrm{Tr}[\mathcal{P}^-_{\mathbf{k},r} \Lambda^e_\mathbf{k}]. \tag{79}$$

They will become obvious in Sec. IV, where we discuss the specific phases in detail. The only nontrivial phase with respect to these identities is the A phase, where $\mathcal{P}^+_{\mathbf{k},r} \neq \mathcal{P}^-_{\mathbf{k},r}$. In this case, one uses Eqs. (B13) from Appendix B to prove these relations.

We arrive at

$$\begin{aligned} \langle \ell_k \rangle_{\hat{\mathbf{k}}} \phi_{k,r} = \frac{g^2}{4} \int \frac{d^3q}{(2\pi)^3} \sum_s \frac{\phi_{q,s} \ell_q}{\epsilon_{\mathbf{q},s}} \tanh\!\left(\frac{\epsilon_{\mathbf{q},s}}{2T}\right) \\ \times \left\langle F_\ell(p) \frac{\ell_k}{\ell_q} \mathcal{T}^s_{00}(\mathbf{k},\mathbf{q}) \right. \\ \left. + F_t(p, \epsilon_{\mathbf{q},s}, \epsilon_{\mathbf{k},r}) \frac{\ell_k}{\ell_q} \mathcal{T}^s_t(\mathbf{k},\mathbf{q}) \right\rangle_{\hat{\mathbf{k}}}, \end{aligned} \tag{80}$$

where we pulled the factor ℓ_q out of the $\hat{\mathbf{k}}$ integral on the right-hand side of the equation. This turns out to be convenient for the calculation. On the left-hand side we have made use of the assumption that the function $\phi_{k,r}$ does not depend on the direction of $\mathbf{k}$. We shall see below that this assumption is consistent with our final result.

Now the angular integral over $\hat{\mathbf{k}}$ has to be performed for each phase separately. In Appendix C we present this calculation explicitly for the transverse polar, planar, and A phases, and in Appendix D it is presented for arbitrary longitudinal phases. However, we can give a general result similar to the method introduced in Ref. [19]. For the angular integral we use a frame with z' axis parallel to $\mathbf{q}$. However, besides the fixed direction given by $\mathbf{q}$, in all nontrivial cases there is another preferred direction in the system, namely, the one that is picked by the order parameter. This has to be taken into account for the integral and is explained in detail in Appendices C and D. We neglect the $\hat{\mathbf{k}}$ dependence in $\epsilon_{\mathbf{k},r}$ occurring in the function F_t. Within this approximation, the functions F_ℓ, F_t do not depend on the azimuthal angle φ', they only enter the $\hat{\mathbf{k}}$ integral through the polar angle θ'. The θ' integral can be transformed into an integral over p. This p integral is performed using the formalism presented in Ref. [19]. To subleading order, we may set $k \simeq q \simeq \mu$, which allows us, for all phases we consider, to write the result of the azimuthal integral in the following power series of p:

$$\frac{1}{2\pi}\int_0^{2\pi} d\varphi' \frac{\ell_k}{\ell_q}\mathcal{T}^s_{00}(\mathbf{k},\mathbf{q}) \simeq a_s\left(\eta_0^\ell + \eta_2^\ell \frac{p^2}{\mu^2} + \eta_4^\ell \frac{p^4}{\mu^4}\right), \tag{81a}$$

$$\frac{1}{2\pi}\int_0^{2\pi} d\varphi' \frac{\ell_k}{\ell_q}\mathcal{T}^s_{t}(\mathbf{k},\mathbf{q}) \simeq a_s\left(\eta_0^t + \eta_2^t \frac{p^2}{\mu^2} + \eta_4^t \frac{p^4}{\mu^4}\right). \tag{81b}$$

The coefficients a_s are chosen such that they add up to one cf. Eq. (8). In all cases we consider, we find

$$a_s = \frac{n_s \lambda_{q,s}}{\sum_r n_r \lambda_{q,r}}, \tag{82}$$

and there are at most two nonzero coefficients a_1, a_2. In general, the coefficients a_s and $\eta^{\ell,t}$ depend on the polar angle θ of the vector $\hat{\mathbf{q}}$ ($\cos\theta = \hat{\mathbf{q}}\cdot\mathbf{e}_z$). However, in most of the cases we consider, they are constant. The only phase with angular-dependent coefficients $\eta^{\ell,t}$ is the mixed polar phase, while the only phase with angular-dependent coefficients a_s is the transverse A phase.

With $\eta_0^\ell = \eta_0^t = 2/3$, which holds for all phases we consider, we arrive at (for details of the p integral, see Ref. [19])

$$\langle \ell_k\rangle_{\hat{\mathbf{k}}}\phi_{k,r} = \int\frac{d\Omega_q}{4\pi}\ell_q \bar{g}^2\int_0^\delta d(q-\mu)\sum_s a_s\frac{\phi_{q,s}}{\epsilon_{\mathbf{q},s}}\frac{1}{2} \times \ln\left(\frac{\tilde{b}^2\mu^2 e^{-2d}}{|\epsilon^2_{\mathbf{q},s}-\epsilon^2_{\mathbf{k},r}|}\right), \tag{83}$$

with $\tilde{b}$ as defined in Eq. (6). The value of d can be determined from the coefficients in Eqs. (81),

$$d = -\frac{6}{\eta_0^t}[\eta_2^\ell + \eta_2^t + 2(\eta_4^\ell + \eta_4^t)]. \tag{84}$$

Consequently, the result of the $\hat{\mathbf{k}}$ integral in the gap equation can be obtained by computing the coefficients of the power series in p, since the p integral is generic for all phases. This result is very similar to that of Ref. [19], where the $\mathbf{q}$ integral on the right-hand side of the gap equation could be performed directly because of the trivial angular structure. In the present, more general, case, however, the $\mathbf{q}$ integral still has to be done. In Eq. (83), this integral has been divided into its angular part and the integral over the modulus q, which can be restricted to an integral over a small region of size 2δ around the Fermi surface, where δ is much larger than the gap but much smaller than the chemical potential. This integral can now be done in the usual way, keeping the angular dependence in the excitation energy $\epsilon_{\mathbf{q},s}$. We briefly repeat this calculation, which leads to Eq. (91), more details for the case of two different gaps can be found in Ref. [19]. With the approximation [16]

$$\frac{1}{2}\ln\left(\frac{\tilde{b}^2\mu^2 e^{-2d}}{|\epsilon^2_{\mathbf{q},s}-\epsilon^2_{\mathbf{k},r}|}\right) \simeq \Theta(\epsilon_{\mathbf{q},s}-\epsilon_{\mathbf{k},r})\ln\left(\frac{\tilde{b}\mu e^{-d}}{\epsilon_{\mathbf{q},s}}\right) + \Theta(\epsilon_{\mathbf{k},r}-\epsilon_{\mathbf{q},s})\ln\left(\frac{\tilde{b}\mu e^{-d}}{\epsilon_{\mathbf{k},r}}\right) \tag{85}$$

and the new variables

$$x_r \equiv \bar{g}\ln\left(\frac{2\tilde{b}\mu e^{-d}}{k-\mu+\epsilon_{\mathbf{k},r}}\right), \qquad y_s \equiv \bar{g}\ln\left(\frac{2\tilde{b}\mu e^{-d}}{q-\mu+\epsilon_{\mathbf{q},s}}\right), \tag{86}$$

to subleading order the gap equation (83) transforms into

$$\langle \ell_k\rangle_{\hat{\mathbf{k}}}\phi(x_r) = \int\frac{d\Omega_q}{4\pi}\ell_q\sum_s a_s\left\{x_r\int_{x_r}^{x_s^*} dy_s \tanh\left[\frac{\epsilon(y_s)}{2T}\right]\phi(y_s) + \int_{x_0}^{x_r} dy_s y_s \tanh\left[\frac{\epsilon(y_s)}{2T}\right]\phi(y_s)\right\}, \tag{87}$$

where we defined

$$x_s^* \equiv \bar{g}\ln\left(\frac{2\tilde{b}\mu e^{-d}}{\sqrt{\lambda_{q,s}}\phi_0}\right), \qquad x_0 \equiv \bar{g}\ln\left(\frac{\tilde{b}\mu e^{-d}}{\delta}\right), \tag{88}$$

with $\phi_0 \equiv \phi(x_1^*) \simeq \phi(x_2^*)$. In the case of an isotropic gap, ϕ_0 is the value of the gap at the Fermi surface. Note that Eq. (87) corresponds to Eq. (79) of Ref. [19]. The difference to that equation, besides the angular integral, arises from the simplification we made above by omitting the wave function renormalization factor.

While Eq. (83) in principle is a set of two equations, one for each excitation branch, labeled by the index r, we see from Eq. (87), that, after the change of variables and neglecting subsubleading contributions, one equation for the variable x_r is left. We can write this single equation for the renamed variable x in the form

$$\langle \ell_k\rangle_{\hat{\mathbf{k}}}\phi(x) = \int\frac{d\Omega_q}{4\pi}\ell_q\left\{x\int_x^{x_2^*} dy \tanh\left[\frac{\epsilon(y)}{2T}\right]\phi(y) + \int_{x_0}^{x} dy y \tanh\left[\frac{\epsilon(y)}{2T}\right]\phi(y) - a_1 x\int_{x_1^*}^{x_2^*} dy \tanh\left[\frac{\epsilon(y)}{2T}\right]\phi(y)\right\}. \tag{89}$$

The solution of this gap equation for $T = 0$ is found in the usual way. Differentiating twice with respect to x yields a second-order differential equation. The two constants of the general solution are determined with the help of Eq. (89) and its first derivative at the point $x = x_2^*$. One obtains

$$\phi(x) = \phi_0[\cos(x_2^* - x) + a_1(x_2^* - x_1^*)\sin(x_2^* - x)]. \tag{90}$$

An exchange of the indices 1 and 2 in this solution yields the same final result for ϕ_0. In order to determine ϕ_0, one inserts the solution (90) into Eq. (89) and evaluates the equation at the point $x = x_2^*$. Then, the integrals on the

right-hand side of the equation are trivial. Using $\sin(\alpha-\beta)=\sin\alpha\cos\beta-\cos\alpha\sin\beta$ and $\cos(\alpha-\beta)=\cos\alpha\cos\beta+\sin\alpha\sin\beta$ and the approximations $\sin x_0\simeq x_0$, $\cos x_0\simeq 1$ [note that x_0 is parametrically of order $O(\bar{g})$], we obtain

$$0=\int\frac{d\Omega_q}{4\pi}\ell_q[\cos x_2^*+a_1(x_2^*-x_1^*)\sin x_2^*], \tag{91}$$

where $\langle\ell_k\rangle_{\hat{\mathbf{k}}}=\langle\ell_q\rangle_{\hat{\mathbf{q}}}$ has been subtracted on both sides of the equation. With the definition for x_2^* in Eq. (88) and the approximations

$$\cos x_2^*\simeq\cos\left[\bar{g}\ln\left(\frac{2\tilde{b}\mu}{\phi_0}\right)\right]+\bar{g}(\ln\sqrt{\lambda_{q,2}}+d)\sin\left[\bar{g}\ln\left(\frac{2\tilde{b}\mu}{\phi_0}\right)\right], \tag{92a}$$

$$\sin x_2^*\simeq\sin\left[\bar{g}\ln\left(\frac{2\tilde{b}\mu}{\phi_0}\right)\right]-\bar{g}(\ln\sqrt{\lambda_{q,2}}+d)\cos\left[\bar{g}\ln\left(\frac{2\tilde{b}\mu}{\phi_0}\right)\right], \tag{92b}$$

we find (using $a_1+a_2=1$)

$$0=\cos\left[\bar{g}\ln\left(\frac{2\tilde{b}\mu}{\phi_0}\right)\right]+\bar{g}(\overline{\zeta}+\overline{d})\sin\left[\bar{g}\ln\left(\frac{2\tilde{b}\mu}{\phi_0}\right)\right]. \tag{93}$$

We use the abbreviations

$$\overline{\zeta}\equiv\frac{\langle\ell_q\zeta\rangle_{\hat{\mathbf{q}}}}{\langle\ell_q\rangle_{\hat{\mathbf{q}}}},\qquad \overline{d}\equiv\frac{\langle\ell_q d\rangle_{\hat{\mathbf{q}}}}{\langle\ell_q\rangle_{\hat{\mathbf{q}}}}, \tag{94}$$

with $\zeta=\ln(\lambda_{q,1}^{a_1}\lambda_{q,2}^{a_2})^{1/2}$, as defined in Eq. (7) for isotropic gaps. With Eqs. (78) and (82), we can write $\overline{\zeta}$ in the following simple form:

$$\overline{\zeta}=\frac{1}{2}\frac{\langle n_1\lambda_{q,1}\ln\lambda_{q,1}+n_2\lambda_{q,2}\ln\lambda_{q,2}\rangle_{\hat{\mathbf{q}}}}{\langle n_1\lambda_{q,1}+n_2\lambda_{q,2}\rangle_{\hat{\mathbf{q}}}}. \tag{95}$$

This expression shows that $\overline{\zeta}$ can be determined solely from the spectrum of the matrix $L_{\mathbf{q}}^{+}$ cf. Eqs. (63), (65), and (66).

From Eq. (93) we deduce that, to subleading order (reinserting the factor b_0'),

$$\phi_0=2\tilde{b}b_0'e^{-\overline{d}}e^{-\overline{\zeta}}\mu\exp\left(-\frac{\pi}{2\bar{g}}\right). \tag{96}$$

This result, which is the main result of this paper, is the generalization of Eq. (5). It says that, in the case of anisotropic gaps and/or an angular-dependent value of d, one has to replace the exponents $d\to\overline{d}$, $\zeta\to\overline{\zeta}$. It turns out that in most of the cases we consider, d is a constant number. Only in the mixed polar phase, see Sec. IV, $\overline{d}\neq d$. However, the modification of the other exponent, $\overline{\zeta}$, plays an important and nontrivial role, especially for the determination of the ground state.

In order to compare the result with the corresponding one in the theory of superfluid ^{3}He, we consider the special case of only one gapped (but anisotropic) excitation branch, $\lambda_{q,2}=a_2=0$. In this case,

$$e^{-\overline{\zeta}}\to\frac{1}{\sqrt{\langle\lambda_{q,1}\rangle_{\hat{\mathbf{q}}}}}\exp\left(-\frac{1}{2}\langle\hat{\lambda}_{q,1}\ln\hat{\lambda}_{q,1}\rangle_{\hat{\mathbf{q}}}\right), \tag{97}$$

and the quadratic mean of the gap is given by

$$\overline{\phi}_1=2\tilde{b}b_0'e^{-\overline{d}}\mu\exp\left(-\frac{\pi}{2\bar{g}}\right)\exp\left(-\frac{1}{2}\langle\hat{\lambda}_{q,1}\ln\hat{\lambda}_{q,1}\rangle_{\hat{\mathbf{q}}}\right). \tag{98}$$

In this special case, the exponent involving the angular dependence of the gap is exactly the same as in ^{3}He cf. Eq. (3.63) of Ref. [14].

C. The critical temperature

In order to determine the critical temperature T_c, we proceed similar to the above calculation of the gap: Starting from the gap equation (89), we apply the method presented in Ref. [19] before doing the $d\Omega_q$ integral. The basic assumption is that the shape of the gap function does not change with temperature, i.e., we employ the following factorization of the temperature-dependent gap function:

$$\phi(x,T)\simeq\phi(T)\frac{\phi(x,0)}{\phi_0}, \tag{99}$$

where $\phi(T)\equiv\phi(x_2^*,T)$ is the value of the gap at the Fermi surface at temperature T, and $\phi(x,0)$ is the zero-temperature gap function $\phi(x)$ computed in the last section. This ansatz, inserted into Eq. (89), yields at the Fermi surface

$$\langle\ell_k\rangle_{\hat{\mathbf{k}}}=\int\frac{d\Omega_q}{4\pi}\ell_q\left\{\int_{x_0}^{x_\kappa}dy\,y\tanh\left[\frac{\epsilon(y)}{2T}\right]\frac{\phi(y,0)}{\phi_0}+\int_{x_\kappa}^{x_2^*}dy\,y\tanh\left[\frac{\epsilon(y)}{2T}\right]\frac{\phi(y,0)}{\phi_0}-a_1x\int_{x_1^*}^{x_2^*}dy\tanh\left[\frac{\epsilon(y)}{2T}\right]\frac{\phi(y,0)}{\phi_0}\right\}, \tag{100}$$

where the second integral in Eq. (89) has been divided into two integrals: One running from x_0 to x_κ, with $x_\kappa\equiv x_2^*-\bar{g}\ln(2\kappa)$, $\kappa\gg 1$, and one running from x_κ to x_2^*. In Ref. [19] it is shown how the integrals in the curly brackets on the right-hand side of Eq. (100) are evaluated. The result is

$$0=\int\frac{d\Omega_q}{4\pi}\ell_q\ln\left(\frac{e^\gamma\phi_0}{\pi T_c}\sqrt{\lambda_{q,1}^{a_1}\lambda_{q,2}^{a_2}}\right). \tag{101}$$

This leads to

$$\frac{T_c}{\phi_0}=\frac{e^\gamma}{\pi}e^{\overline{\zeta}}. \tag{102}$$

Note that, although the ratio T_c/ϕ_0 depends on the constant $\overline{\zeta}$, the absolute value for T_c does not, since the factor $e^{-\overline{\zeta}}$ of the gap ϕ_0 cancels the factor $e^{\overline{\zeta}}$ on the right-hand side of Eq. (102). Consequently, in units of the critical temperature in the 2SC phase, T_c^{2SC}, the critical temperature only depends on the constant $\overline{d}$, $T_c/T_c^{\mathrm{2SC}} = e^{-\overline{d}}$.

We recover as a special case the result for two isotropic gaps, Eq. (10). For the case of only one gapped excitation branch, and using Eq. (97), the ratio between the critical temperature and the quadratic mean of the gap at the Fermi surface for $T = 0$ reads

$$\frac{T_c}{\overline{\phi}_1} = \frac{e^{\gamma}}{\pi} \exp\left(\frac{1}{2}\langle \hat{\lambda}_{q,1} \ln \hat{\lambda}_{q,1}\rangle_{\hat{\mathbf{q}}}\right). \tag{103}$$

Consequently, we find a nontrivial modification of the BCS relation $T_c = 0.57\phi_0$ also in the case of a single, but anisotropic gap. Obviously, the BCS relation is recovered from Eq. (103) for the case of a constant gap, since in this case $\hat{\lambda}_{q,1} = 1$. Note that the result (103) is identical to the one in the theory of superfluid ^{3}He cf. Eq. (3.63) of Ref. [14].

D. The pressure

The starting point for the calculation of the pressure is the effective action, Eq. (45). In the two-loop approximation, we can write

$$\Gamma_2[\Delta, S] = \tfrac{1}{4}\mathrm{Tr}(\Sigma S). \tag{104}$$

Then, making use of the Dyson-Schwinger equation (46b), the fermionic part of the effective potential at the stationary point can be written as

$$\Gamma[S] = \tfrac{1}{2}\mathrm{Tr}\ln S^{-1} - \tfrac{1}{4}\mathrm{Tr}(1 - S_0^{-1}S). \tag{105}$$

In order to evaluate the first term on the right-hand side of this equation, we use the identity $\mathrm{Tr}\ln S^{-1} = \ln\det S^{-1}$ and the fact that for arbitrary matrices $\mathcal{A}$, $\mathcal{B}$, C, and an invertible matrix $\mathcal{D}$,

$$\det\begin{pmatrix} \mathcal{A} & \mathcal{B} \\ C & \mathcal{D} \end{pmatrix} = \det(\mathcal{A}\mathcal{D} - \mathcal{B}\mathcal{D}^{-1}C\mathcal{D}). \tag{106}$$

Then, making use of $S^{-1} = S_0^{-1} + \Sigma$ and Eqs. (48) and (50), the trace over Nambu-Gor'kov space yields

$$\begin{aligned}\tfrac{1}{2}\mathrm{Tr}\ln S^{-1} = \tfrac{1}{2}\mathrm{Tr}\ln\{&([G_0^+]^{-1} + \Sigma^+)([G_0^-]^{-1} + \Sigma^-) \\ &- \Phi^-([G_0^-]^{-1} + \Sigma^-)^{-1}\Phi^+([G_0^-]^{-1} \\ &+ \Sigma^-)\}.\end{aligned} \tag{107}$$

In order to proceed, we set $Z(k_0) \simeq 1$ in the fermion propagator $G^{\pm}$ cf. its definition in Eq. (61). Using the identity

$$[G_0^{\mp}]^{-1}[G_0^{\pm}]^{-1} = \sum_e [k_0^2 - (\mu - ek)^2]\Lambda_{\mathbf{k}}^{\pm e}, \tag{108}$$

we find

$$\begin{aligned}\frac{1}{2}\mathrm{Tr}\ln S^{-1} &= \frac{1}{2}\mathrm{Tr}\ln\sum_e [k_0^2 - (\mu - ek)^2 - \phi_e^2 L_{\mathbf{k}}^+]\Lambda_{\mathbf{k}}^{-e} \\ &= \frac{1}{2}\sum_{e,r}\sum_K \mathrm{Tr}[\mathcal{P}_{\mathbf{k},r}^+\Lambda_{\mathbf{k}}^{-e}]\ln[k_0^2 - (\epsilon_{\mathbf{k},r}^e)^2].\end{aligned} \tag{109}$$

After performing the Matsubara sum, this expression reads

$$\begin{aligned}\frac{1}{2}\mathrm{Tr}\ln S^{-1} = \frac{1}{2}\frac{V}{T}\sum_{e,r}\int\frac{d^3k}{(2\pi)^3}\,&\mathrm{Tr}[\mathcal{P}_{\mathbf{k},r}^+\Lambda_{\mathbf{k}}^{-e}] \\ &\times\left\{\epsilon_{\mathbf{k},r}^e + 2T\ln\left[1 + \exp\left(-\frac{\epsilon_{\mathbf{k},r}^e}{T}\right)\right]\right\},\end{aligned} \tag{110}$$

where the trace now runs only over color, flavor, and Dirac space.

The Nambu-Gor'kov trace for the second term on the right-hand side of Eq. (105) is easily performed with the definitions (48) and (51). Note that the anomalous propagators $\Xi^{\pm}$, occurring in the full quark propagator S, do not enter the result. One obtains

$$\begin{aligned}\frac{1}{4}\mathrm{Tr}(1 - S_0^{-1}S) = -\frac{1}{4}\sum_{e,r}\sum_K \mathrm{Tr}[&\mathcal{P}_{\mathbf{k},r}^+\Lambda_{\mathbf{k}}^e + \mathcal{P}_{\mathbf{k},r}^-\Lambda_{\mathbf{k}}^{-e}] \\ &\times\frac{\lambda_{k,r}\phi_e^2}{k_0^2 - (\epsilon_{\mathbf{k},r}^e)^2},\end{aligned} \tag{111}$$

which becomes, after performing the Matsubara sum,

$$\begin{aligned}\frac{1}{4}\mathrm{Tr}(1 - S_0^{-1}S) = \frac{1}{4}\frac{V}{T}\sum_{e,r}\int\frac{d^3k}{(2\pi)^3}\,&\times\mathrm{Tr}[\mathcal{P}_{\mathbf{k},r}^+\Lambda_{\mathbf{k}}^e + \mathcal{P}_{\mathbf{k},r}^-\Lambda_{\mathbf{k}}^{-e}] \\ &\times\frac{\lambda_{k,r}\phi_e^2(\epsilon_{\mathbf{k},r}^e, k)}{2\epsilon_{\mathbf{k},r}}\tanh\frac{\epsilon_{\mathbf{k},r}^e}{2T}.\end{aligned} \tag{112}$$

Using Eq. (79), the final result for the pressure $p = -V_{\mathrm{eff}} = \frac{T}{V}\Gamma$, obtained by putting together Eqs. (110) and (112), is

$$\begin{aligned}p = \frac{1}{4}\sum_{e,r}\int\frac{d^3k}{(2\pi)^3}\,&\mathrm{Tr}[\mathcal{P}_{\mathbf{k},r}^+]\left\{\epsilon_{\mathbf{k},r}^e + 2T\ln\left[1 + \exp\left(-\frac{\epsilon_{\mathbf{k},r}^e}{T}\right)\right]\right. \\ &\left. - \frac{\lambda_{k,r}\phi_e^2(\epsilon_{\mathbf{k},r}^e, k)}{2\epsilon_{\mathbf{k},r}^e}\tanh\frac{\epsilon_{\mathbf{k},r}^e}{2T}\right\}.\end{aligned} \tag{113}$$

In the following, we restrict ourselves to the zero-temperature case, $T = 0$. Furthermore, we neglect the antiparticle gap and thus denote $\phi \equiv \phi_+$, as above. In this case, Eq. (113) becomes

$$p = \frac{1}{4}\sum_r\int\frac{d^3k}{(2\pi)^3}\,n_r\left(\epsilon_{\mathbf{k},r}^+ + \epsilon_{\mathbf{k},r}^- - \frac{\lambda_{k,r}\phi_{k,r}^2}{2\epsilon_{\mathbf{k},r}^+}\right). \tag{114}$$

In order to evaluate the integral over the absolute value of the quark momentum, we assume the gap function to be constant in a small region around the Fermi surface of size

2δ, $\phi_{k,r} = \phi_0$, and zero elsewhere. Moreover, we use the integrals

$$\int_0^\delta d\xi\left(\sqrt{\xi^2+\phi_0^2}-\frac{1}{2}\frac{\phi_0^2}{\sqrt{\xi^2+\phi_0^2}}\right)=\frac{1}{2}\delta\sqrt{\delta^2+\phi_0^2}$$
$$=\frac{1}{2}\delta^2+\frac{1}{4}\phi_0^2+O\left(\frac{\phi_0^4}{\delta^2}\right), \tag{115}$$

and

$$\int_0^\infty dk k^2(\epsilon_{k0}^+ + \epsilon_{k0}^- - 2k) = \frac{1}{6}\mu^4, \tag{116}$$

where the vacuum energy $2k$ has been subtracted and $\epsilon_{k0}^e \equiv |k - e\mu|$. Neglecting terms of order $O(\phi_0^4)$, we find

$$p = \frac{\mu^4}{48\pi^2}\sum_r n_r + \Delta p, \tag{117}$$

where we denote the difference of the superconducting phase to that of the normal phase by

$$\Delta p = \frac{\mu^2}{16\pi^2}\sum_r n_r \overline{\phi}_r^2. \tag{118}$$

As expected from physical intuition and from the theory of ^{3}He cf. Eq. (1), the favored phase is determined by the largest condensation energy Δp, which is proportional to the sum of the angular averages of the squares of the gap, weighted with the corresponding degeneracies n_r of the excitation branches. (Note that, since $\overline{\phi}_r = \sqrt{\langle\lambda_{k,r}\rangle_{\hat{\mathbf{k}}}}\phi_0$ is the *quadratic mean* of the gap, $\overline{\phi}_r^2 = \langle\lambda_{k,r}\rangle_{\hat{\mathbf{k}}}\phi_0^2$ is the angular average of the square of the gap, not the square of the angular average, as the notation might suggest.)

As a special case, one finds for the 2SC phase, counting Dirac, color, and flavor degrees of freedom,

$$\Delta p_{\mathrm{2SC}} = \frac{\mu^2(\phi_0^{\mathrm{2SC}})^2 N_f}{2\pi^2}. \tag{119}$$

This is in accordance with Ref. [31], when one identifies the pressure with the negative value of the effective potential at the global minimum.

IV. DISCUSSION OF THE POLAR, PLANAR, A, AND CSL PHASES

In this section, we use the general results of the previous sections for a discussion of the physical properties of certain phases in a spin-one color superconductor. In particular, we determine the ground state at zero temperature. We focus on the four ''inert'' phases presented in Sec. II, the polar, planar, A, and CSL phases, see Fig. 1.

The common structure of all spin-one phases is given by the matrix $\mathcal{M}_{\mathbf{k}}$, that determines the color and Dirac structure of the gap matrix $\Phi^+(K)$, Eq. (58). The most general form of this matrix has been introduced in Eq. (17). Specifying the spin-triplet structure κ_j, we write the matrix as

$$\mathcal{M}_{\mathbf{k}} = \sum_{i,j=1}^{3} J_i \Delta_{ij}[\alpha\hat{k}_j + \beta\gamma_{\perp,j}(\mathbf{k})]. \tag{120}$$

The first term in angular brackets, proportional to the jth component of the fermion momentum unit vector $\hat{k}_j$, describes pairing of quarks with the same chirality, since it commutes with the chirality projector $\mathcal{P}_{r,\ell} = (1 \pm \gamma_5)/2$. The second one, proportional to

$$\gamma_{\perp,j}(\hat{\mathbf{k}}) \equiv \gamma_j - \hat{k}_j\boldsymbol{\gamma}\cdot\hat{\mathbf{k}}, \qquad j = 1, 2, 3, \tag{121}$$

corresponds to pairing of quarks of opposite chirality, since commuting this term with the chirality projector flips the sign of chirality. In the above ansatz for the gap matrix we allow for a general linear combination of these two terms, determined by the real coefficients α and β with

$$\alpha^2 + \beta^2 = 1. \tag{122}$$

In Refs. [11,19] the special cases $(\alpha, \beta) = (1, 0)$ and $(\alpha, \beta) = (0, 1)$ were termed longitudinal and transverse gaps, respectively. We shall also use these terms in the following. (In Ref. [12], the LL and RR gaps correspond to the longitudinal and the LR and RL gaps to the transverse gaps.) The reason why both cases can be studied separately is that a purely longitudinal gap matrix on the right-hand side of the gap equation does not induce a transverse gap on the left-hand side and vice versa. More precisely, inserting the matrix $\mathcal{M}_{\mathbf{k}}$ from Eq. (120) with $\beta = 0$ into the anomalous propagator from Eq. (70), and the result into the right-hand side of the gap equation (56), we realize that the Dirac structure still commutes with γ_5 and thus preserves chirality. The analogous argument holds for the transverse gap, $\alpha = 0$. For the case of an equal admixture of longitudinal and transverse gaps, i.e., $\alpha = \beta = 1/\sqrt{2}$, let us use the term mixed gap. For the physical results, we focus exclusively on the longitudinal, mixed, and transverse gaps.

We summarize the relevant quantities for the different phases in Tables I, II, III, and IV. The physically important results are collected in Tables V, VI, and VII and Fig. 2.

Let us first comment on Tables I, II, III, and IV. For the planar and A phases, we use the abbreviations

$$A_{1/2} \equiv (\alpha^2 - \beta^2)\hat{k}_{1/2}^2 + \beta^2, \tag{123a}$$
$$B \equiv (\alpha^2 - \beta^2)\hat{k}_1\hat{k}_2, \tag{123b}$$
$$Z \equiv \beta\{\alpha[\hat{k}_2\gamma_{\perp,1}(\hat{\mathbf{k}}) - \hat{k}_1\gamma_{\perp,2}(\hat{\mathbf{k}})] - \beta[\gamma_{\perp,1}(\hat{\mathbf{k}})\gamma_{\perp,2}(\hat{\mathbf{k}}) - \hat{k}_1\hat{k}_2]\}. \tag{123c}$$

The quantities $A_{1/2}$, B, and Z are diagonal in color space. But while $A_{1/2}$ and B are scalars, Z is a nontrivial 4×4 matrix in Dirac space. One can verify the relation

TABLE I. Relevant quantities for the polar phase.

$$\mathcal{M}_{\mathbf{k}} = J_3[\alpha\hat{k}_3 + \beta\gamma_{\perp,3}(\hat{\mathbf{k}})]$$
$$L^{\pm}_{\mathbf{k}} = J_3^2[\beta^2 + (\alpha^2 - \beta^2)\cos^2\theta]$$
$$\lambda_{k,1} = \beta^2 + (\alpha^2 - \beta^2)\cos^2\theta \ (n_1 = 8),\ \lambda_{k,2} = 0 \ (n_2 = 4)$$
$$\mathcal{P}^{\pm}_{\mathbf{k},1} = J_3^2,\ \mathcal{P}^{\pm}_{\mathbf{k},2} = 1 - J_3^2$$

	Longitudinal	Mixed	Transverse
$\lambda_{k,r}$ (n_r)	$\cos^2\theta$ (8), 0 (4)	1/2 (8), 0 (4)	$\sin^2\theta$ (8), 0 (4)
a_r	1, 0	1, 0	1, 0
$\overline{d}$	6	5	9/2
$\overline{\zeta}$	$-1/3$	$-\ln\sqrt{2}$	$\ln 2 - 5/6$

TABLE II. Relevant quantities for the planar phase.

$$\mathcal{M}_{\mathbf{k}} = J_1[\alpha\hat{k}_1 + \beta\gamma_{\perp,1}(\hat{\mathbf{k}})] + J_2[\alpha\hat{k}_2 + \beta\gamma_{\perp,2}(\hat{\mathbf{k}})]$$
$$L^{\pm}_{\mathbf{k}} = J_1^2 A_1 + J_2^2 A_2 + \{J_1, J_2\}B + [J_1, J_2]Z$$
$$\lambda_{k,1} = \alpha^2\sin^2\theta + \beta^2(1 + \cos^2\theta) \ (n_1 = 8),\ \lambda_{k,2} = 0 \ (n_2 = 4)$$
$$\mathcal{P}^{\pm}_{\mathbf{k},1} = L^{\pm}_{\mathbf{k}}/\lambda_{k,1},\ \mathcal{P}^{\pm}_{\mathbf{k},2} = 1 - L^{\pm}_{\mathbf{k}}/\lambda_{k,1}$$

	Longitudinal	Mixed	Transverse
$\lambda_{k,r}$ (n_r)	$\sin^2\theta$ (8), 0 (4)	1 (8), 0 (4)	$1 + \cos^2\theta$ (8), 0 (4)
a_r	1, 0	1, 0	1, 0
$\overline{d}$	6	21/4	9/2
$\overline{\zeta}$	$\ln 2 - 5/6$	0	$\ln\sqrt{2} - 7/12 + \pi/8$

$$Z^2 = B^2 - A_1 A_2. \tag{124}$$

Moreover, in the table for the planar phase, we denote the anticommutator by $\{-, -\}$. The angle θ, used in Tables I, II, and III is the angle between the quark momentum $\mathbf{k}$ and the z axis. The indices $a, b \leq 3$ in the second line of Table IV are color indices.

The specific form of the matrices $\mathcal{M}_{\mathbf{k}}$ is obtained by inserting the respective order parameters Δ cf. Fig. 1, into the definition (120). The matrices $L^{\pm}_{\mathbf{k}}$ are given by the definition (63). The calculation of their eigenvalues $\lambda_{k,r}$ and corresponding degeneracies n_r is presented in Appendix B for the planar and A phases. The same method can be applied to the other phases, see for instance Refs. [19,29]. After determining the eigenvalues, the corresponding projectors are obtained with the help of Eq. (64). All these quantities, $\mathcal{M}_{\mathbf{k}}$, $L^{\pm}_{\mathbf{k}}$, $\lambda_{k,r}$, n_r, and $\mathcal{P}^{\pm}_{\mathbf{k},r}$, are computed for arbitrary linear combinations of longitudinal and transverse gaps and are given in the first four lines of Tables I, II, III, and IV. The last four lines of these tables are devoted to the special cases of pure longitudinal and transverse gaps and the mixed gap. First, we present the eigenvalues $\lambda_{k,r}$ with the corresponding degeneracies, immediately deduced from the general ones. Then, we compute the quantities a_r, see Eqs. (81), and $\overline{d}$, see Eqs. (84) and (94). The calculation of these quantities is more or less straightforward, but may turn out to be lengthy. It involves performing the color and Dirac traces in the quantities $\mathcal{T}^{s}_{00}(\mathbf{k}, \mathbf{q})$ and $\mathcal{T}^{s}_{i}(\mathbf{k}, \mathbf{q})$ as well as the angular integration over $\hat{\mathbf{k}}$, see Eq. (80). For the most complicated cases, the transverse polar, planar, and A

TABLE III. Relevant quantities for the A phase.

$$\mathcal{M}_{\mathbf{k}} = J_3\{\alpha(\hat{k}_1 + i\hat{k}_2) + \beta[\gamma_{\perp,1}(\hat{\mathbf{k}}) + i\gamma_{\perp,2}(\hat{\mathbf{k}})]\}$$
$$L^{\pm}_{\mathbf{k}} = J_3^2[(A_1 + A_2) \pm 2iZ]$$
$$\lambda_{k,1/2} = \alpha^2\sin^2\theta + \beta^2(1 + \cos^2\theta) \pm 2\beta\sqrt{\alpha^2\sin^2\theta + \beta^2\cos^2\theta} \ (n_1 = n_2 = 4),\ \lambda_{k,3} = 0 \ (n_3 = 4)$$
$$\mathcal{P}^{\pm}_{\mathbf{k},1} = \tfrac{1}{2}J_3^2[1 \pm (i/\sqrt{A_1A_2 - B^2})Z],\ \mathcal{P}^{\pm}_{\mathbf{k},2} = \tfrac{1}{2}J_3^2[1 \mp (i/\sqrt{A_1A_2 - B^2})Z],\ \mathcal{P}^{\pm}_{\mathbf{k},3} = 1 - J_3^2$$

	Longitudinal	Mixed	Transverse
$\lambda_{k,r}$ (n_r)	$\sin^2\theta$ (8), 0 (4)	2 (4), 0 (8)	$(1 + \lvert\cos\theta\rvert)^2$ (4), $(1 - \lvert\cos\theta\rvert)^2$ (4), 0 (4)
a_r	1, 0	1, 0	$1/2 + \lvert\cos\theta\rvert/(1 + \cos^2\theta)$, $1/2 - \lvert\cos\theta\rvert/(1 + \cos^2\theta)$, 0
$\overline{d}$	6	21/4	9/2
$\overline{\zeta}$	$\ln 2 - 5/6$	$\ln\sqrt{2}$	$\ln 2 - 1/3$

TABLE IV. Relevant quantities for the CSL phase.

$$\mathcal{M}_{\mathbf{k}} = \mathbf{J}\cdot[\alpha\hat{\mathbf{k}} + \beta\boldsymbol{\gamma}_{\perp}(\hat{\mathbf{k}})]$$
$$(L^{\pm}_{\mathbf{k}})_{ab} = (\alpha^2+2\beta^2)\delta_{ab} - [\alpha\hat{k}_b + \beta\gamma_{\perp,b}(\hat{\mathbf{k}})][\alpha\hat{k}_a - \beta\gamma_{\perp,a}(\hat{\mathbf{k}})]$$
$$\lambda_{k,1/2} = \tfrac{1}{2}\alpha^2 + 2\beta^2 \pm \tfrac{1}{2}\alpha\sqrt{\alpha^2+8\beta^2}\ (n_1=n_2=4),\ \lambda_{k,3} = \alpha^2\ (n_3=4)$$
$$\mathcal{P}^{\pm}_{\mathbf{k},r} = \textstyle\prod_{s\neq r}^{3}(L^{\pm}_{\mathbf{k}} - \lambda_{k,s})/(\lambda_{k,r}-\lambda_{k,s})$$

	Longitudinal	Mixed	Transverse
$\lambda_{k,r}$ (n_r)	1 (8), 0 (4)	2 (4), 1/2 (8)	2 (8), 0 (4)
a_r	1, 0	2/3, 1/3	1, 0
$\overline{d}$	6	5	9/2
$\overline{\zeta}$	0	$\ln\sqrt{2^{1/3}}$	$\ln\sqrt{2}$

TABLE V. Gap functions $\sqrt{\lambda_{k,r}}\phi_0$ in units of the 2SC gap. Figure 2 illustrates this table schematically.

$\sqrt{\lambda_{k,r}}\phi_0/\phi_0^{\mathrm{2SC}}$	Longitudinal	Mixed	Transverse
Polar	$\lvert\cos\theta\rvert e^{1/3}e^{-6}$	e^{-5}	$\lvert\sin\theta\rvert\frac{1}{2}e^{5/6}e^{-9/2}$
Planar	$\lvert\sin\theta\rvert\frac{1}{2}e^{5/6}e^{-6}$	$e^{-21/4}$	$\sqrt{1+\cos^2\theta}\frac{1}{\sqrt{2}}e^{7/12-\pi/8}e^{-9/2}$
A	$\lvert\sin\theta\rvert\frac{1}{2}e^{5/6}e^{-6}$	$e^{-21/4}$	$(1\pm\lvert\cos\theta\rvert)\frac{1}{2}e^{1/3}e^{-9/2}$
CSL	e^{-6}	$2^{(-1\pm3)/6}e^{-5}$	$e^{-9/2}$

TABLE VI. The critical temperature T_c in units of the critical temperature for the 2SC phase.

T_c/T_c^{2SC}	Longitudinal	Mixed	Transverse
Polar	e^{-6}	e^{-5}	$e^{-9/2}$
Planar	e^{-6}	$e^{-21/4}$	$e^{-9/2}$
A	e^{-6}	$e^{-21/4}$	$e^{-9/2}$
CSL	e^{-6}	e^{-5}	$e^{-9/2}$

TABLE VII. Zero-temperature pressure Δp (condensation energy) in units of the 2SC pressure. The results are illustrated in Fig. 2.

$\Delta p/\Delta p_{\mathrm{2SC}}$	Longitudinal	Mixed	Transverse
Polar	$\frac{1}{3}e^{2/3}e^{-12} \simeq 0.65e^{-12}$	e^{-10}	$\frac{1}{6}e^{5/3}e^{-9} \simeq 0.88e^{-9}$
Planar	$\frac{1}{6}e^{5/3}e^{-12} \simeq 0.88e^{-12}$	$e^{-21/2}$	$\frac{2}{3}e^{7/6-\pi/4}e^{-9} \simeq 0.98e^{-9}$
A	$\frac{1}{6}e^{5/3}e^{-12} \simeq 0.88e^{-12}$	$\frac{1}{2}e^{-21/2}$	$\frac{1}{3}e^{2/3}e^{-9} \simeq 0.65e^{-9}$
CSL	e^{-12}	$3\times 2^{-4/3}e^{-10}$	e^{-9}

phases, we present details of the calculation in Appendix C. Furthermore, in Appendix D it is shown that $\overline{d} = d = 6$ is a universal result for all longitudinal phases. A special case is the mixed polar phase, which is the only case where d turns out to be angular dependent, $d = 3(3+\cos^2\theta)/2$. This result has already been obtained in Refs. [19,29]. However, it has not been realized that $\overline{d} = 5$, and not d, enters the value of the gap ϕ_0. Finally, the constant $\overline{\zeta}$ is straightforwardly obtained by using Eqs. (7) and (94).

Let us now turn to the physically important results, Tables V, VI, and VII and Fig. 2. In Table V we present the (angular-dependent) gap functions for zero temperature at the Fermi surface, as they occur in the quasiparticle energies, Eq. (67). They involve the square root of the eigenvalue $\lambda_{k,r}$ and the factors $e^{-\overline{d}}$ and $e^{-\overline{\zeta}}$, as shown in the solution of the gap equation cf. Eq. (96). The results are easily computed using the results of the previous tables. The magnitude of the gaps are reduced compared to the gaps in the spin-zero phases by factors of the order $e^{-6} \simeq 2.4\times10^{-3}$ through $e^{-9/2} \simeq 1.1\times10^{-2}$. Consequently, assuming the spin-zero gaps to be of the order of 10 MeV, the spin-one gaps are of the order of 10–100 keV.

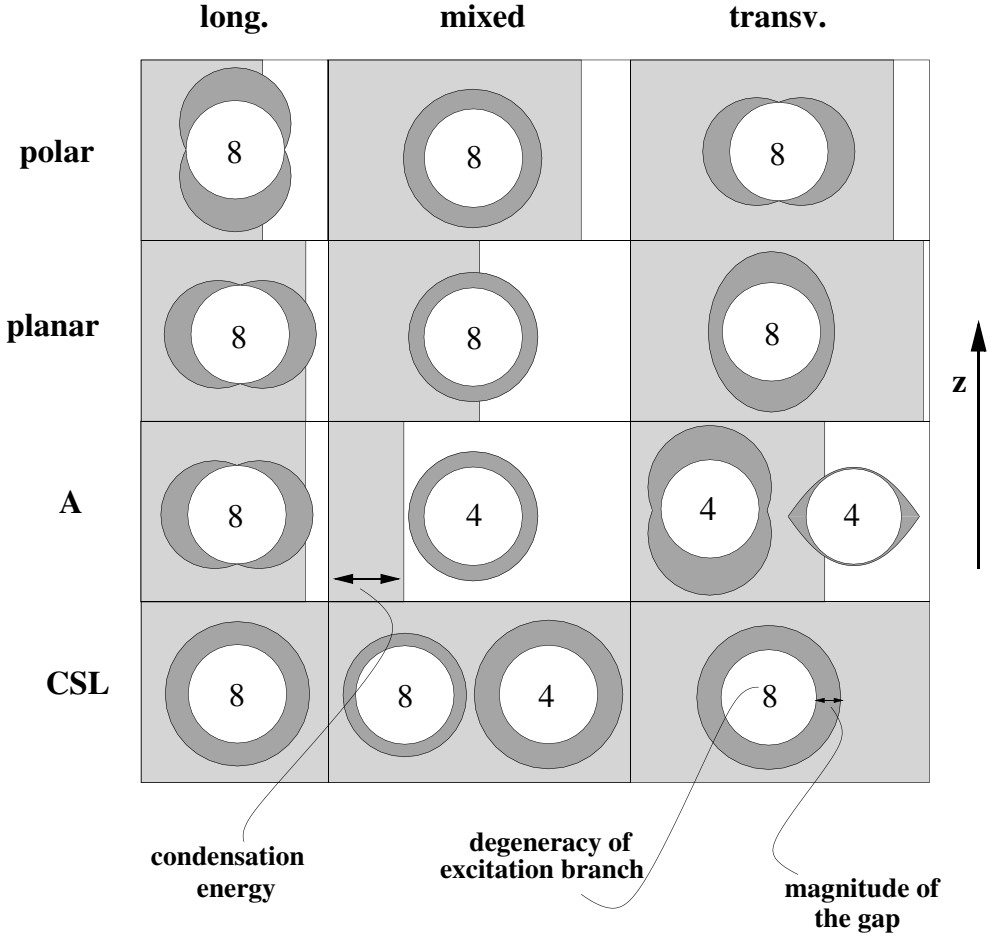

FIG. 2. Schematic representation of the gap functions $\sqrt{\lambda_{r,k}}\phi_0$, given in Table V, and condensation energies, given in Table VII. All gap functions are symmetric with respect to rotations around the z axis. The numbers correspond to the degeneracies of the respective excitation branches. Only the gapped excitations are shown. The condensation energies are drawn to scale in each column separately.

The angular structure of the gap functions, given in Table V, is illustrated in Fig. 2. In this figure, the magnitude of the gap at the Fermi surface is shown as a function of the polar angle θ. None of the functions depends on the azimuthal angle φ, i.e., all figures are symmetric with respect to rotations around the z axis. First note that the gaps in the CSL phase are isotropic. Nevertheless, there is a hidden anisotropy also in this phase, since the residual symmetry is not the group of rotations in real space but the group of joint rotations in color and real space. Thus, analogous to the B phase in ^{3}He one might call this phase ''pseudoisotropic.'' Other analogies to ^{3}He can be found, particularly in the first column of the figure, representing the longitudinal gaps. All structures correspond to their analogues in ^{3}He. This is plausible, because the respective gap matrices do not involve the nontrivial Dirac part $\boldsymbol{\gamma}_\perp(\hat{\mathbf{k}})$, and thus can, in this respect, be considered as the nonrelativistic limit. Note that the longitudinal polar phase has a nodal line at the equator of the Fermi sphere, while the longitudinal planar and A phases have nodal points at the north and south pole of the Fermi sphere. All longitudinal phases have one gapped and one ungapped excitation branch with degeneracies 8 and 4, respectively, cf. Appendix D. Note that the degeneracies add up to 12, since the matrix $L^+_{\mathbf{k}}$ is a 12×12 matrix, involving antiparticle degrees of freedom. Nevertheless, the physical degeneracies of the gapped branches have to be reduced by a factor 2 compared to Fig. 2, since the antiparticle gaps are negligibly small.

All phases shown in the second and third columns of the figure have no analogues in ^{3}He, because $\boldsymbol{\gamma}_\perp(\hat{\mathbf{k}})$ gives rise to a nontrivial Dirac structure. The mixed gaps all are isotropic. The transverse gaps, however, exhibit nontrivial angular structures. The transverse polar phase has point nodes, similar to the longitudinal planar and A phases. The transverse planar phase has an anisotropic gap, however, the gap vanishes nowhere. The transverse A phase has one ungapped excitation and two different gapped ones, each with a nontrivial angular structure. One of these structures has no nodes but minima at the equator of the Fermi sphere, while the other has point nodes at the north and the south pole.

The critical temperatures, presented in Table VI, are obtained from Eq. (102). As remarked below that equation, the absolute value of T_c depends only on the factor $e^{-\overline{d}}$. Therefore, the results of Table VI are easy to interpret. The constant $\overline{d}$ assumes the value $\overline{d} = 6$ for all longitudinal gaps, which therefore all have the same transition temperature, being of the order of 10 keV (again applying $\phi_0^{2SC} \simeq 10$ MeV). Since the mixed phases have different values for $\overline{d}$, their transition temperatures differ, ranging in the order 30–40 keV. The transverse phases have the largest transition temperature, $T_c \simeq 60$ keV.

The most important physical results of this paper can be found in Table VII, and, schematically, in Fig. 2, since they answer the question of the preferred state in a spin-one color superconductor at zero temperature. Crucial to this question is the factor $e^{-\overline{\zeta}}$ in the gap function, which is strongly affected by the nontrivial angular structures in the gap equation, which was not realized in Ref. [29], where a simple approximation for the angular integral had been used. The first obvious result, already indicated by the results of Ref. [12] and independent of the constant $\overline{\zeta}$, is that the pressure of all transverse phases is larger than that of the mixed phases, which, in turn, is larger than that of the longitudinal phases. Therefore, the most interesting and relevant phases are the transverse ones. Nevertheless, let us mention that in the results for the longitudinal phases we recover Eq. (2), i.e., the ratio between the condensation energies of the longitudinal A and CSL phases is identical to the corresponding one of the A and B phases in ^{3}He. For the transverse phases, the result cannot be anticipated from the theory of ^{3}He. We find that the condensation energy of the phases with nodal lines or points of the gap, i.e., the polar and A phases, is smaller than that of the phases without nodes. However, note that the polar phase has a larger condensation energy than the A phase, although it has more excitation branches with nodes in the gap function (eight compared to four). The two phases without zeros in the gap function, i.e., the planar and CSL phases, differ only by 2% in their condensation energy. The isotropic transverse CSL phase has the largest condensation energy.

Note that electric charge neutrality of the system does not affect the results, since we are considering a one-flavor system. This, of course, is in contrast to the systems where quarks of different flavors form Cooper pairs. In these systems, for instance in the (gapless) 2SC and CFL phases, charge neutrality plays an important role regarding the question of the ground state. The effect of the condition of *color* charge neutrality for a one-flavor system is less trivial. In the polar and A phases, Cooper pairs carry color charge antiblue, i.e., only red and green quarks condense while the blue quarks remain unpaired. This pattern is known from the 2SC phase. It leads to a nonvanishing expectation value of the gluon field A_8^μ [32], which ensures color neutrality of the system. This is equivalent to introducing a color chemical potential μ_8 [6] which discriminates between the chemical potentials for paired and unpaired quarks. In the planar phase, Cooper pairs are formed by red/blue and green/blue quarks, i.e., they carry color charge antigreen or antired. Also in this case, one expects the color chemical potential for red and green quarks to differ from that for the blue quarks because of the residual color group $SU(2)$. Consequently, quarks of different chemical potentials form Cooper pairs. In both cases, the condition of color neutrality might reduce the pressure. In contrast, the CSL phase automatically fulfills color neutrality, since there are equal numbers of Cooper pairs with colors antired, antigreen, and antiblue. Therefore, the result that the transverse CSL phase has the largest pressure is insensitive with respect to electric and color neutrality conditions.

V. SUMMARY AND OUTLOOK

In this paper, we have investigated the possible color-superconducting phases in cold and dense quark matter, where quarks of the same flavor form Cooper pairs, which leads to Cooper pairs with total spin one. It has been argued that these phases might be relevant in the interior of neutron stars, since a mismatch of Fermi surfaces, if too large, forbids pairing of quarks of different flavors. Since the structure of the order parameter of the spin-one phases corresponds to a complex 3×3 matrix, *a priori* a multitude of phases seems to be possible. It has been the main goal of this paper to pick the order parameter that leads to the phase with the largest pressure, indicating that it is the favored spin-one color superconductor. In principle, this task is comparable to the three-flavor case, where the CFL phase turns out to be the favored one. However, in that case, the argument that favors the CFL phase is more or less obvious and plausible, since it is the only possible phase in which all quasiparticles attain a gap in their excitation spectrum. The present paper shows that for the spin-one phases the argument is more subtle, since, in particular, it involves the angular structures of the gap functions. Angular-dependent gap functions are known from condensed-matter systems, for instance from superfluid ^{3}He. We have shown that a certain class of spin-one phases, named longitudinal phases (where quarks of the same chirality form Cooper pairs), reproduces some features of the phases in ^{3}He, namely, the angular structure and the relative condensation energies of the several phases. However, most of the investigated phases, and, in particular, the preferred transverse phases (where quarks of opposite chirality form Cooper pairs), have no analogues in ^{3}He.

The specific technical and physical results of the paper can be summarized as follows. In the systematic classification of order parameters, based on group-theoretical arguments, we have found four phases with uniquely defined order parameter matrices. These phases, the polar,

planar, A, and CSL phases, all break color and rotational symmetries. From the theory of ^{3}He we transfer the conclusion that these order parameters correspond to the inert phases, although the different group structure in principle demands for a more careful investigation of this statement. Nevertheless, we have picked the above mentioned four phases for a more detailed discussion. Before evaluating these phases specifically, we have presented a general solution of the QCD gap equation. This treatment generalizes the one presented in Ref. [19]. The main conclusion is that an angular dependence of the gap function gives rise to a nontrivial factor $e^{-\overline{\zeta}}$ in the expression for the zero-temperature gap. The explicit result of the gap is

$$\phi_0 = 2\tilde{b}b_0' e^{-\overline{d}} e^{-\overline{\zeta}} \mu \exp\left(-\frac{\pi}{2\bar{g}}\right). \tag{125}$$

It generalizes Eq. (5) by the replacements

$$\zeta \to \overline{\zeta} \equiv \frac{\langle \ell_q \zeta \rangle_{\hat{\mathbf{q}}}}{\langle \ell_q \rangle_{\hat{\mathbf{q}}}}, \qquad d \to \overline{d} \equiv \frac{\langle \ell_q d \rangle_{\hat{\mathbf{q}}}}{\langle \ell_q \rangle_{\hat{\mathbf{q}}}}. \tag{126}$$

The quantity ℓ_q is (half of) the sum of the eigenvalues $\lambda_{k,r}$ of the matrix $L_{\mathbf{k}}^+$ cf. Eq. (78). These eigenvalues contain the angular structure of the gaps. According to Eq. (95), $\overline{\zeta}$ can be determined solely from the quasiparticle spectrum. The physical meaning of the replacement $\zeta \to \overline{\zeta}$ can be illustrated as follows. Consider an isotropic gap function, ϕ, and an anisotropic one, say $|\sin\theta|\phi$, where θ is the angle between the quark momentum and one fixed spatial axis. One would immediately conclude that the condensation energy of the former one is larger, since the latter assumes its maximum value ϕ only for $\theta = \pi/2$, while it is reduced for all other angles. However, we have found that the latter one actually is equipped with the above mentioned factor, i.e., it reads $|\sin\theta| e^{-\overline{\zeta}} \phi$. If $e^{-\overline{\zeta}} > 1$, the question of the preferred phase is nontrivial and depends on the special value of $\overline{\zeta}$. The general result presented here reproduces the special cases of one or two isotropic gaps.

Furthermore, we have computed a general expression for the critical temperature,

$$\frac{T_c}{\phi_0} = \frac{e^\gamma}{\pi} e^{\overline{\zeta}}. \tag{127}$$

This equation shows that the BCS relation $T_c/\phi_0 \simeq 0.57$ is not only violated in the cases of a two-gap structure and a gapless color superconductor. It is also violated in the case of a single gapped excitation branch if the corresponding gap is anisotropic. In this case, the ratio between the critical temperature and the quadratic mean $\overline{\phi}$ of the gap is given by Eq. (103), which is exactly the same result as for ^{3}He.

Finally, a general expression of the pressure at zero temperature has been derived starting from the effective action, which can be obtained from the QCD partition function using the CJT formalism. In particular, the pressure contains the condensation energy (density), which is the difference of the pressure in the superconducting phase compared to the normal-conducting phase,

$$\Delta p = \frac{\mu^2}{16\pi^2} \sum_r n_r \overline{\phi}_r^2. \tag{128}$$

Physically, this result is plausible. It is equivalent to counting the gapped branches and weight them with the angular average of the square of the corresponding gaps. Again, our general result reproduces the well-known results for the spin-zero gaps.

These general results for the gap, the critical temperature, and the pressure have been applied to the above mentioned four spin-one phases. The genuinely new results concern all phases with nontrivial angular structure. These are the longitudinal and transverse polar, planar, and A phases, while the pseudoisotropic CSL phase already has been discussed in Refs. [12,19]. It has been shown that several of the phases exhibit nodal points or lines of the gap, similar to ^{3}He and several high-T_c superconductors in condensed-matter physics [33]. The magnitude of the gap is dominated by the factor $e^{-\overline{d}}$ which varies from e^{-6} for longitudinal gaps to $e^{-9/2}$ for transverse gaps. These factors have already been found in Refs. [12,17]. The consequence is that the spin-one gaps are smaller by 2–3 orders of magnitude than the spin-zero gaps, which renders them of the order of 10–100 keV. These numbers are not changed essentially by the factor $e^{-\overline{\zeta}}$ which, in all cases, is of order one. Nevertheless, this factor is decisive for the question of the favored phase, which can be found among the transverse phases. Since the pressure of all transverse phases contains the factor e^{-9} and since the number of the gapped excitation branches in all transverse phases equals 8, the preferred phase is determined by the specific factors originating from the angular structure. The result is that the transverse CSL phase has the largest pressure. This phase has an isotropic energy gap, contrary to all other transverse phases. It has been discussed that this result remains unchanged under the condition of overall color charge neutrality.

Let us finally add some remarks regarding astrophysical consequences. As a first result, we note that the existence of a spin-one color superconductor in the interior of a neutron star is not ruled out by the temperatures, which, in the case of old neutron stars, is in the range of keV. In order to find consequences of a spin-one color-superconducting core for the observables of the neutron star, it seems to be very promising to study the interplay of the superconductor with the magnetic field of the star. In Refs. [21,22] it has been discussed in detail that the mixed polar as well as the mixed CSL phase exhibit an electromagnetic Meissner effect, contrary to the spin-zero phases. From these results one concludes that it is very likely that also the other spin-one phases expel electromagnetic fields,

although an explicit calculation has not yet been done. For the transverse CSL phase, this statement is obvious due to its symmetry breaking pattern. It might be interesting to investigate whether the angular structure, in particular, the nodal points or lines, leads to anisotropies regarding external magnetic fields, for instance to angular-dependent penetration depths. Furthermore, external magnetic fields should be included into the discussion of the favored phase. As we know from ^{3}He, above a certain threshold for the external magnetic field, the B phase is no longer the ground state of the system. Instead, the anisotropic A phase becomes favored. Therefore, it remains a physically important project for the future to investigate if the CSL phase is still preferred in the presence of a magnetic field.

Another measurable property of a neutron star which is likely to be affected by a color-superconducting core is its temperature, or, more precisely, its cooling curve (temperature as a function of time) [34]. Recently, it has been argued, that, unlike a spin-zero color superconductor, a spin-one color superconductor could explain the observed cooling curves [35]. The main ingredient of this conclusion has been the magnitude of the gap, i.e., the keV gap compared to the MeV gap of the 2SC or CFL phases. The physical mechanism behind this cooling curve is the emission of neutrinos, which dominates the cooling of the star after the first few seconds after its creation. Since one of the involved processes of neutrino emission is the Urca process, which requires the breaking of a Cooper pair, it might be interesting to take into account not only the effect of the magnitude but also of the nodal structure of the gap. Moreover, the nodes of the gap function would certainly affect the specific heat of the system. Note for instance that in the A phase of ^{3}He (which has the same nodal structure as the longitudinal A phase in a spin-one color superconductor), the specific heat depends on temperature according to a power law, while in the B phase the temperature dependence of the specific heat shows an exponential behavior. Similar effects can be expected for a spin-one color superconductor and have to be included into a careful discussion of the cooling behavior of a neutron star.

ACKNOWLEDGMENTS

I thank D. H. Rischke for valuable suggestions and a careful reading of the manuscript. I thank T. Schäfer, I. A. Shovkovy, and Q. Wang for valuable discussions and comments.

APPENDIX A: ORDER PARAMETERS CORRESPONDING TO RESIDUAL GROUPS $H = U(1) \times H'$

In this appendix, we evaluate the invariance equation (25). This means that we determine all possible residual subgroups of the form $H = U(1) \times H'$ and the corresponding order parameters, using Eq. (24) as an ansatz for the generator for the residual $U(1)$. The invariance condition can be written as a system of nine equations,

$$\left(-\frac{a_8}{2\sqrt{3}} + 2c\right)\Delta_{11} + ib_3\Delta_{12} = 0, \tag{A1a}$$

$$\left(-\frac{a_8}{2\sqrt{3}} + 2c\right)\Delta_{12} - ib_3\Delta_{11} = 0, \tag{A1b}$$

$$\left(-\frac{a_8}{2\sqrt{3}} + 2c\right)\Delta_{13} = 0, \tag{A1c}$$

$$\left(-\frac{a_8}{2\sqrt{3}} + 2c\right)\Delta_{21} + ib_3\Delta_{22} = 0, \tag{A1d}$$

$$\left(-\frac{a_8}{2\sqrt{3}} + 2c\right)\Delta_{22} - ib_3\Delta_{21} = 0, \tag{A1e}$$

$$\left(-\frac{a_8}{2\sqrt{3}} + 2c\right)\Delta_{23} = 0, \tag{A1f}$$

$$\left(-\frac{a_8}{\sqrt{3}} + 2c\right)\Delta_{31} + ib_3\Delta_{32} = 0, \tag{A1g}$$

$$\left(-\frac{a_8}{\sqrt{3}} + 2c\right)\Delta_{32} - ib_3\Delta_{31} = 0, \tag{A1h}$$

$$\left(-\frac{a_8}{\sqrt{3}} + 2c\right)\Delta_{33} = 0. \tag{A1i}$$

The corresponding coefficient matrix A exhibits a block structure and the determinant thus factorizes into four subdeterminants. Therefore, we have to consider the equation

$$0 = \det A = \det A_1 \det A_2 \det A_3 \det A_4, \tag{A2}$$

where

$$\det A_1 = \left[\left(-\frac{a_8}{2\sqrt{3}} + 2c\right)^2 - b_3^2\right]^2, \tag{A3a}$$

$$\det A_2 = \left(-\frac{a_8}{2\sqrt{3}} + 2c\right)^2, \tag{A3b}$$

$$\det A_3 = \left(\frac{a_8}{\sqrt{3}} + 2c\right)^2 - b_3^2, \tag{A3c}$$

$$\det A_4 = \frac{a_8}{\sqrt{3}} + 2c. \tag{A3d}$$

Now, one can systematically list all possibilities that yield a zero determinant of the coefficient matrix and thus allow for a nonzero order parameter.

(1) $\det A_1 = 0$.

Here we distinguish between the cases (i) where the two terms in the angular brackets of Eq. (A3a) cancel each other and (ii) where they separately vanish.

(i) a_8, c arbitrary, $b_3 = -a_8/(2\sqrt{3}) + 2c$.

Inserting these conditions for the coefficients into Eqs. (A1), one obtains for the order parameter matrix

$$\Delta = \frac{1}{N}\begin{pmatrix} \Delta_1 & i\Delta_1 & 0 \\ \Delta_2 & i\Delta_2 & 0 \\ 0 & 0 & 0 \end{pmatrix}, \qquad \text{(A4)}$$

where the factor $1/N$ with $N = (2|\Delta_1|^2 + 2|\Delta_2|^2)^{1/2}$ accounts for the normalization (26). In this case, the order parameter contains two independent parameters Δ_1 and Δ_2. From this form of the order parameter, we can now determine the group H' in Eq. (22). Inserting Δ into Eq. (21) and using the fact that the parameters Δ_1, Δ_2 are independent of each other, one obtains the conditions

$$\begin{aligned} &a_1 = \ldots = a_7 = b_1 = b_2 = 0, \\ &\frac{1}{2\sqrt{3}}a_8 + b_3 - 2c = 0. \end{aligned} \qquad \text{(A5)}$$

Consequently,

$$H = U(1) \times U(1), \qquad \text{(A6)}$$

since a vanishing coefficient in Eq. (A5) translates to a "broken dimension" of G. For instance, $a_1 = 0$ means that T_1 does not occur in the generators of H, etc. The dimensions of the residual Lie group can be counted with the help of the number of the conditions for the coefficients. Since $\dim G = \dim G_1 + \dim G_2 + \dim G_3 = 8 + 3 + 1 = 12$, and the number of conditions in Eqs. (A5) is 10, we conclude $\dim H = 2$, which is in agreement with Eq. (A6). Or, in other words, there is an additional $U(1)$, i.e., $H' = U(1)$ in Eq. (22) because the equation relating the three coefficients a_8, b_3, c allows for two linearly independent generators U and V which are linear combinations of the generators T_8, J_3, $\mathbf{1}$. Note that U and V are not uniquely determined. One possible choice is

$$U = T_8 - \frac{1}{2\sqrt{3}}J_3, \qquad V = 2J_3 + \mathbf{1}. \qquad \text{(A7)}$$

Different order parameters are obtained from two subcases:

First, one can impose the additional relation $c = -a_8/(2\sqrt{3})$ between the two coefficients that have been arbitrary above. Then, $b_3 = -a_8\sqrt{3}/2$. These two conditions yield

$$\Delta = \frac{1}{N}\begin{pmatrix} \Delta_1 & i\Delta_1 & 0 \\ \Delta_2 & i\Delta_2 & 0 \\ 0 & 0 & \Delta_3 \end{pmatrix}, \qquad \text{(A8)}$$

where $N = (2|\Delta_1|^2 + 2|\Delta_2|^2 + |\Delta_3|^2)^{1/2}$. In this case, Eq. (21) leads to 11 conditions for the coefficients a_m, b_n, c, which leaves a subgroup

$$H = U(1), \qquad \text{(A9)}$$

generated by a linear combination of generators of all three original subgroups G_1, G_2, G_3,

$$U = T_8 - \frac{\sqrt{3}}{2}J_3 - \frac{1}{2\sqrt{3}}\mathbf{1}. \qquad \text{(A10)}$$

Second, one can set one of the coefficients a_8, c to zero. The condition $c = 0$ does not yield a new case. But $a_8 = 0$, and consequently $b_3 = 2c$, has to be treated separately. In this case, Eqs. (A1) yield

$$\Delta = \frac{1}{N}\begin{pmatrix} \Delta_1 & i\Delta_1 & 0 \\ \Delta_2 & i\Delta_2 & 0 \\ \Delta_3 & i\Delta_3 & 0 \end{pmatrix}, \qquad \text{(A11)}$$

where $N = (2|\Delta_1|^2 + 2|\Delta_2|^2 + 2|\Delta_3|^2)^{1/2}$. The residual group is given by

$$H = U(1), \qquad \text{(A12)}$$

generated by

$$U = 2J_3 + \mathbf{1}. \qquad \text{(A13)}$$

(ii) $c = a_8/(4\sqrt{3})$, $b_3 = 0$.
Here, one obtains

$$\Delta = \frac{1}{N}\begin{pmatrix} \Delta_1 & \Delta_2 & \Delta_3 \\ \Delta_4 & \Delta_5 & \Delta_6 \\ 0 & 0 & 0 \end{pmatrix}, \qquad \text{(A14)}$$

where $N = (\sum_{i=1}^{6} |\Delta_i|^2)^{1/2}$. Again, the residual group is one-dimensional,

$$H = U(1), \qquad \text{(A15)}$$

generated by

$$U = T_8 + \frac{1}{4\sqrt{3}}\mathbf{1}. \qquad \text{(A16)}$$

(2) $\det A_2 = 0$.
This determinant vanishes in the following cases:
(i) b_3 arbitrary, $c = a_8/(4\sqrt{3})$.
With Eqs. (A1), one obtains

$$\Delta = \frac{1}{N}\begin{pmatrix} 0 & 0 & \Delta_1 \\ 0 & 0 & \Delta_2 \\ 0 & 0 & 0 \end{pmatrix}, \qquad \text{(A17)}$$

where $N = (|\Delta_1|^2 + |\Delta_2|^2)^{1/2}$. Inserting Δ into Eq. (21) yields

$$a_1 = \ldots = a_7 = b_1 = b_2 = 0, \qquad c = \frac{1}{4\sqrt{3}} a_8. \tag{A18}$$

As for the order parameter (A4), the residual group is given by

$$H = U(1) \times U(1). \tag{A19}$$

However, the corresponding generators differ from those in Eqs. (A7),

$$U = T_8 + \frac{1}{4\sqrt{3}}\mathbf{1}, \qquad V = J_3. \tag{A20}$$

(ii) b_3 arbitrary, $a_8 = c = 0$.
In this case,

$$\Delta = \frac{1}{N}\begin{pmatrix} 0 & 0 & \Delta_1 \\ 0 & 0 & \Delta_2 \\ 0 & 0 & \Delta_3 \end{pmatrix}, \tag{A21}$$

where $N = (|\Delta_1|^2 + |\Delta_2|^2 + |\Delta_3|^2)^{1/2}$. The residual group is

$$H = U(1), \tag{A22}$$

which is a subgroup of the spin group $G_2 = SU(2)_J$, since it is generated by

$$U = J_3. \tag{A23}$$

(3) $\det A_3 = 0$.
(i) a_8, c arbitrary, $b_3 = a_8/\sqrt{3} + 2c$.
In this case, we find with Eqs. (A1),

$$\Delta = \frac{1}{\sqrt{2}}\begin{pmatrix} 0 & 0 & 0 \\ 0 & 0 & 0 \\ 1 & i & 0 \end{pmatrix}. \tag{A24}$$

This matrix differs from all previously discussed order parameters in that it is uniquely determined. It corresponds to the A phase. Here, as in all cases above, we omitted a possible phase factor which could multiply Δ without violating the normalization. Inserting Δ into Eqs. (21) yields the following relations:

$$a_4 = \ldots = a_7 = b_1 = b_2 = 0, \qquad \frac{1}{\sqrt{3}} a_8 - b_3 + 2c = 0. \tag{A25}$$

Consequently, besides the relation between a_8, b_3, and c, there are only six additional conditions. Thus, the dimension of the residual group is $12 - 7 = 5$. We obtain

$$H = SU(2) \times U(1) \times U(1), \tag{A26}$$

where $SU(2)$ is generated by T_1, T_2, T_3, and thus is a subgroup of the color gauge group $G_1 = SU(3)_c$. For the generators of the two $U(1)$'s one can choose

$$U = T_8 - \frac{1}{2\sqrt{3}}\mathbf{1}, \qquad V = J_3 + \mathbf{1}. \tag{A27}$$

As in case 1(i), there is a subcase that produces an additional order parameter. Namely, if we require the condition $c = a_8/(4\sqrt{3})$, which yields $b_3 = \sqrt{3}a_8/2$, we obtain

$$\Delta = \frac{1}{N}\begin{pmatrix} 0 & 0 & \Delta_2 \\ 0 & 0 & \Delta_3 \\ \Delta_1 & i\Delta_1 & 0 \end{pmatrix}, \tag{A28}$$

where $N = (2|\Delta_1|^2 + |\Delta_2|^2 + |\Delta_3|^2)^{1/2}$. From Eqs. (A1) we conclude that all other coefficients vanish. Consequently,

$$H = U(1), \tag{A29}$$

with the generator

$$U = T_8 + \frac{\sqrt{3}}{2} J_3 + \frac{1}{4\sqrt{3}}\mathbf{1}. \tag{A30}$$

(ii) $b_3 = 0$, $c = -a_8/(2\sqrt{3})$.
With Eqs. (A1) one obtains

$$\Delta = \frac{1}{N}\begin{pmatrix} 0 & 0 & 0 \\ 0 & 0 & 0 \\ \Delta_1 & \Delta_2 & \Delta_3 \end{pmatrix}, \tag{A31}$$

where N is defined as in Eq. (A21). From Eq. (21) we conclude in this case

$$a_4 = \ldots = a_7 = b_1 = b_2 = b_3 = 0, \qquad c = -\frac{a_8}{2\sqrt{3}}. \tag{A32}$$

Hence, the residual group is

$$H = SU(2) \times U(1), \tag{A33}$$

generated by T_1, T_2, T_3, and

$$U = T_8 - \frac{1}{2\sqrt{3}}\mathbf{1}. \tag{A34}$$

(4) $\det A_4 = 0$.
There are two cases in which $\det A_4 = 0$:
(i) b_3 arbitrary, $c = -a_8/(2\sqrt{3})$.
These relations lead to

$$\Delta = \begin{pmatrix} 0 & 0 & 0 \\ 0 & 0 & 0 \\ 0 & 0 & 1 \end{pmatrix}, \tag{A35}$$

As in the A phase, Eq. (A24), the order parameter is uniquely determined. It describes the polar phase. Inserting the order parameter of the polar phase into the invariance condition, Eq. (21), yields

$$a_4 = \ldots = a_7 = b_1 = b_2 = 0, \qquad c = -\frac{1}{2\sqrt{3}} a_8. \tag{A36}$$

Therefore, the residual group is

$$H = SU(2) \times U(1) \times U(1) \tag{A37}$$

with the generators T_1, T_2, T_3, and

$$U = T_8 - \frac{1}{2\sqrt{3}}\mathbf{1}, \qquad V = J_3. \tag{A38}$$

Thus, the symmetry breaking pattern in the polar phase is similar to that in the A phase cf. (A27). But while in the A phase both residual $U(1)$'s are combinations of the original symmetries, in the polar phase, one of them is a subgroup of $G_2 = SU(2)_J$.

(ii) b_3 arbitrary, $a_8 = c = 0$.
This case is identical to case 2(ii).

APPENDIX B: EIGENVALUES OF $L_{\mathbf{k}}^{\pm}$ IN THE PLANAR AND A PHASES

1. Planar phase

In order to compute the eigenvalues of the matrix $L_{\mathbf{k}}^{+} = L_{\mathbf{k}}^{-}$, given in Table II, we use Eq. (124) and the (anti)-commutation properties of the color matrices $(J_i)_{jk} = -i\epsilon_{ijk}$ to obtain $(L_{\mathbf{k}}^{\pm})^2 = (A_1 + A_2)L_{\mathbf{k}}^{\pm}$. Therefore,

$$(L_{\mathbf{k}}^{\pm})^n = (A_1 + A_2)^{n-1} L_{\mathbf{k}}^{\pm}. \tag{B1}$$

This simple relation for the nth power of $L_{\mathbf{k}}^{\pm}$ can be used to find the roots of the equation

$$\det(\lambda - L_{\mathbf{k}}^{\pm}) = 0, \tag{B2}$$

which yield the eigenvalues λ of $L_{\mathbf{k}}^{\pm}$. Since

$$\det(\lambda - L_{\mathbf{k}}^{\pm}) \equiv \exp[\mathrm{Tr}\ln(\lambda - L_{\mathbf{k}}^{\pm})], \tag{B3}$$

we consider the trace of the logarithm of $\lambda - L_{\mathbf{k}}^{\pm}$,

$$\mathrm{Tr}\ln(\lambda - L_{\mathbf{k}}^{\pm}) = \ln\lambda\,\mathrm{Tr}\mathbf{1} + \mathrm{Tr}\ln\left(\mathbf{1} - \frac{L_{\mathbf{k}}^{\pm}}{\lambda}\right) = \ln\lambda\,\mathrm{Tr}\mathbf{1} - \sum_{n=1}^{\infty}\frac{1}{n}\lambda^{-n}\,\mathrm{Tr}(L_{\mathbf{k}}^{\pm})^n. \tag{B4}$$

The second term on the right-hand side can be evaluated using Eq. (B1). With $\mathrm{Tr}L_{\mathbf{k}}^{\pm} = 8(A_1 + A_2)$ one obtains

$$\det(\lambda - L_{\mathbf{k}}^{\pm}) = \lambda^4[\lambda - (A_1 + A_2)]^8, \tag{B5}$$

which yields the eigenvalues $A_1 + A_2$ and 0 with degeneracies 8 and 4, respectively. With the definition (123a), this confirms the entries for $\lambda_{k,r}$ in Table II.

2. A phase

In order to derive an expression for the nth power of the matrix $L_{\mathbf{k}}^{\pm}$, given in Table III, we note that

$$(L_{\mathbf{k}}^{\pm})^2 = 2(A_1 + A_2)L_{\mathbf{k}}^{\pm} - [(A_1 - A_2)^2 + 4B^2]J_3^2, \tag{B6}$$

where Eq. (124) has been used. Since $A_{1/2}$ and B are scalars and $J_3^2 L_{\mathbf{k}}^{\pm} = L_{\mathbf{k}}^{\pm}$, we have

$$(L_{\mathbf{k}}^{\pm})^n = a_n L_{\mathbf{k}}^{\pm} + b_n J_3^2, \tag{B7}$$

with real coefficients a_n, b_n. Applying Eq. (B6), one derives the following recursion relations for these coefficients:

$$a_{n+1} = 2(A_1 + A_2)a_n + b_n, \qquad b_{n+1} = -[(A_1 - A_2)^2 + 4B^2]a_n. \tag{B8}$$

With the ansatz of a power series, $a_n = p^n$, one obtains a quadratic equation for p, which has the two solutions

$$p_{1/2} = A_1 + A_2 \pm 2\sqrt{A_1A_2 - B^2}. \tag{B9}$$

Therefore, a_n is a linear combination of the nth powers of these solutions, $a_n = \eta_1 p_1^n + \eta_2 p_2^n$. The coefficients η_1, η_2 can be determined from $a_1 = 1$, $a_2 = 2(A_1 + A_2)$. One finds

$$a_n = \frac{1}{4}\frac{1}{\sqrt{A_1A_2 - B^2}}(p_1^n - p_2^n), \qquad b_n = -\frac{1}{4}\frac{(A_1 - A_2)^2 + 4B^2}{\sqrt{A_1A_2 - B^2}}(p_1^{n-1} - p_2^{n-1}). \tag{B10}$$

With $\mathrm{Tr}L_{\mathbf{k}}^{\pm} = 8(A_1 + A_2)$ this yields

$$\det(\lambda - L_{\mathbf{k}}^{\pm}) = \lambda^4(\lambda - p_1)^4(\lambda - p_2)^4. \tag{B11}$$

Consequently, both $L_{\mathbf{k}}^{+}$ and $L_{\mathbf{k}}^{-}$ have the eigenvalues 0, p_1, and p_2, each with degeneracy 4, which confirms the corresponding entries in Table III.

Finally, we consider the projectors $\mathcal{P}_{\mathbf{k},r}^{\pm}$ corresponding to the eigenvalues λ. With

$$\mathcal{P}_{\mathbf{k},1/2}^{\pm} = \frac{L_{\mathbf{k}}^{\pm}(L_{\mathbf{k}}^{\pm} - \lambda_{2/1})}{\lambda_{1/2}(\lambda_{1/2} - \lambda_{2/1})}, \qquad \mathcal{P}_{\mathbf{k},3}^{\pm} = \mathbf{1} - \mathcal{P}_{\mathbf{k},1}^{\pm} - \mathcal{P}_{\mathbf{k},2}^{\pm}, \tag{B12}$$

one obtains

$$\mathcal{P}_{\mathbf{k},1}^{\pm} = \frac{1}{2}J_3^2\left(1 \pm \frac{i}{\sqrt{A_1A_2 - B^2}}Z\right), \tag{B13a}$$

$$\mathcal{P}_{\mathbf{k},2}^{\pm} = \frac{1}{2}J_3^2\left(1 \mp \frac{i}{\sqrt{A_1A_2 - B^2}}Z\right), \tag{B13b}$$

$$\mathcal{P}_{\mathbf{k},3}^{\pm} = 1 - J_3^2. \tag{B13c}$$

Since $\mathrm{Tr}Z = \mathrm{Tr}(\Lambda^e_{\mathbf{k}} Z) = 0$, Eq. (79) is obviously fulfilled also in the A phase.

APPENDIX C: TRACES AND ANGULAR INTEGRALS FOR THE TRANSVERSE PHASES

In this appendix, we present the technical details of the solution of the gap equation for the transverse polar, planar, and A phases. The transverse CSL phase is trivial with respect to the angular structure and has already been discussed in Ref. [19]. We compute the color and Dirac traces and perform the $\hat{\mathbf{k}}$ integration of Eq. (80) in order to determine the coefficients a_s and $\eta^{\ell,t}$ introduced in Eqs. (81). These coefficients yield the constant d cf. Eq. (84).

Let us define the following traces over Dirac space:

$$\mathcal{Q}^{mn}_{\mu\nu} \equiv \mathrm{Tr}[\gamma_\mu \gamma_{\perp,m}(\hat{\mathbf{q}}) \Lambda^-_{\mathbf{q}} \gamma_\nu \gamma_{\perp,n}(\hat{\mathbf{k}}) \Lambda^+_{\mathbf{k}}], \tag{C1a}$$

$$\mathcal{R}^{mn}_{\mu\nu} \equiv \mathrm{Tr}[\gamma_\mu \gamma_{\perp,m}(\hat{\mathbf{q}}) \gamma_0\gamma_5 \boldsymbol{\gamma}\cdot\hat{\mathbf{q}} \Lambda^-_{\mathbf{q}} \gamma_\nu \gamma_{\perp,n}(\hat{\mathbf{k}}) \Lambda^+_{\mathbf{k}}]. \tag{C1b}$$

We shall make use of the following results:

$$\mathcal{Q}^{mn}_{00} = -\delta_{mn}(1 + \hat{\mathbf{q}}\cdot\hat{\mathbf{k}}) + \hat{k}_m\hat{k}_n + \hat{q}_m\hat{q}_n - \hat{q}_m\hat{k}_n\hat{\mathbf{q}}\cdot\hat{\mathbf{k}} + \hat{q}_n\hat{k}_m, \tag{C2a}$$

$$(\delta^{ij} - \hat{p}^i\hat{p}^j)\mathcal{Q}^{mn}_{ij} = 2[-\hat{p}_m\hat{p}_n + \hat{q}_n\hat{k}_m - \hat{\mathbf{q}}\cdot\hat{\mathbf{k}}(\delta_{mn} - \hat{p}_m\hat{p}_n) + \hat{p}_m(\hat{k}_n - \hat{q}_n)\hat{\mathbf{p}}\cdot\hat{\mathbf{k}} - \hat{p}_n(\hat{k}_m - \hat{q}_m)\hat{\mathbf{p}}\cdot\hat{\mathbf{q}} + (\delta_{mn} - \hat{q}_m\hat{k}_n)\hat{\mathbf{p}}\cdot\hat{\mathbf{q}}\,\hat{\mathbf{p}}\cdot\hat{\mathbf{k}}], \tag{C2b}$$

$$\mathcal{R}^{12}_{00} - \mathcal{R}^{21}_{00} = i(\hat{q}_3 + \hat{k}_3)(1 + \hat{\mathbf{q}}\cdot\hat{\mathbf{k}}), \tag{C2c}$$

$$(\delta^{ij} - \hat{p}^i\hat{p}^j)(\mathcal{R}^{12}_{ij} - \mathcal{R}^{21}_{ij}) = -2i\{[1 - (\hat{\mathbf{p}}\cdot\hat{\mathbf{k}})^2]\hat{q}_3 + [1 - (\hat{\mathbf{p}}\cdot\hat{\mathbf{q}})^2]\hat{k}_3 - (1 - \hat{\mathbf{q}}\cdot\hat{\mathbf{k}})(\hat{\mathbf{p}}\cdot\hat{\mathbf{k}} + \hat{\mathbf{p}}\cdot\hat{\mathbf{q}})\hat{p}_3\}. \tag{C2d}$$

1. Transverse polar phase

Using the matrix $\mathcal{M}_{\mathbf{k}}$ from Table I with $(\alpha, \beta) = (0, 1)$, we find

$$\mathrm{Tr}[\mathcal{M}_{\mathbf{k}}\mathcal{M}^\dagger_{\mathbf{k}}\Lambda^+_{\mathbf{k}}] = 4(1 - \hat{k}_3^2), \tag{C3}$$

and thus

$$\mathcal{T}^1_{00}(\mathbf{k},\mathbf{q}) = \frac{1}{3(1-\hat{k}_3^2)}[1 + \hat{\mathbf{q}}\cdot\hat{\mathbf{k}} - \hat{q}_3\hat{k}_3(1 - \hat{\mathbf{q}}\cdot\hat{\mathbf{k}}) - \hat{k}_3^2 - \hat{q}_3^2], \tag{C4}$$

where the color trace $\mathrm{Tr}[T_a^T J_3 T_a J_3] = -4/3$ has been used. Analogously, we find

$$\mathcal{T}^1_t(\mathbf{k},\mathbf{q}) = \frac{2}{3(1-\hat{k}_3^2)}[-\hat{q}_3\hat{k}_3 + \hat{\mathbf{q}}\cdot\hat{\mathbf{k}} + \hat{p}_3^2(1 - \hat{\mathbf{q}}\cdot\hat{\mathbf{k}}) - \hat{p}_3(\hat{q}_3 - \hat{k}_3)(\hat{\mathbf{p}}\cdot\hat{\mathbf{q}} - \hat{\mathbf{p}}\cdot\hat{\mathbf{k}}) - (1 - \hat{q}_3\hat{k}_3)\hat{\mathbf{p}}\cdot\hat{\mathbf{q}}\,\hat{\mathbf{p}}\cdot\hat{\mathbf{k}}]. \tag{C5}$$

In order to obtain these results, Eqs. (C2a) and (C2b) with $m = n = 3$ have been employed. As expected, the ungapped excitation branch does not contribute to the gap equation, $\mathcal{T}^2_{00}(\mathbf{k},\mathbf{q}) = \mathcal{T}^2_t(\mathbf{k},\mathbf{q}) = 0$, and thus $a_1 = 1$, $a_2 = 0$.

Next, the angular integral $d\Omega_k$ has to be performed. To this end, we use the following frame (cf. left diagram in Fig. 3): The order parameter in the polar phase picks a special direction in real space. By convention, we choose this direction to be parallel to the z axis. Now there is another fixed direction, $\hat{\mathbf{q}}$, which we can choose to be in the xz plane, $\hat{\mathbf{q}} = (\sin\theta, 0, \cos\theta)$, where θ is the polar angle. In order to perform the $d\Omega_k$ integral, we use a frame with z' axis parallel to $\hat{\mathbf{q}}$. The original frame can be transformed into the new one with a rotation $R(\theta)$ around the y axis,

$$R(\theta) = \begin{pmatrix} \cos\theta & 0 & -\sin\theta \\ 0 & 1 & 0 \\ \sin\theta & 0 & \cos\theta \end{pmatrix}. \tag{C6}$$

In the new frame, we have $\hat{\mathbf{q}}' = (0, 0, 1)$ and $\hat{\mathbf{k}}' = (\sin\theta'\cos\varphi', \sin\theta'\sin\varphi', \cos\theta')$. Therefore, before performing the $d\Omega_k$ integral, we write $\hat{\mathbf{k}}$ as

$$\hat{\mathbf{k}} = R^{-1}(\theta)\hat{\mathbf{k}}' = \begin{pmatrix} \cos\theta\sin\theta'\cos\varphi' + \sin\theta\cos\theta' \\ \sin\theta'\sin\varphi' \\ -\sin\theta\sin\theta'\cos\varphi' + \cos\theta\cos\theta' \end{pmatrix}. \tag{C7}$$

This new frame is particularly convenient, since the new polar angle θ' is the angle between $\hat{\mathbf{q}}$ and $\hat{\mathbf{k}}$, $\cos\theta' = \hat{\mathbf{q}}\cdot\hat{\mathbf{k}}$. Therefore, the integration over θ' can be transformed into an integral over p via $\cos\theta' = (k^2 + q^2 - p^2)/(2kq)$, where p is the modulus of $\mathbf{p} = \mathbf{k} - \mathbf{q}$. Note that the function F_ℓ on the right-hand side of Eq. (80) does not depend on the azimuthal angle φ' but only on p, and the function F_t only depends on p and θ, but not on φ' either (neglecting the $\hat{\mathbf{k}}$ dependence in $\epsilon_{\mathbf{k},r}$). Consequently, we have to multiply $\mathcal{T}^1_{00}$ and $\mathcal{T}^1_t$, given in Eqs. (C4) and (C5), respectively, with the factor $\ell_k/\ell_q = (1 - \hat{k}_3^2)/(1 - \hat{q}_3^2)$, write the results in terms of the new coordinates and integrate over φ'. After setting $k \simeq q \simeq \mu$, which is permissible to subleading order, the result yields the coefficients η in Eq. (81). Then, the result of the p integral is obtained by Eq. (84), following Ref. [19].

The explicit results of this procedure are as follows. With

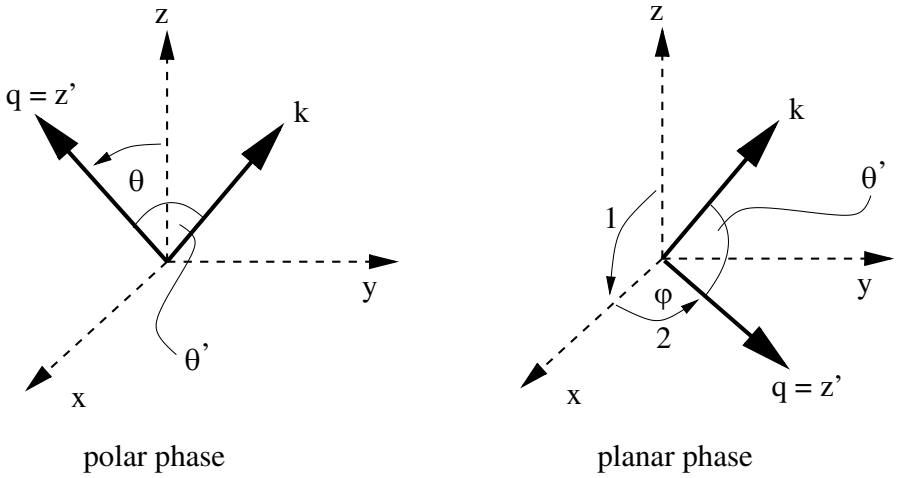

FIG. 3. Rotation of the coordinate system $(x, y, z) \to (x', y', z')$ for the $\hat{\mathbf{k}}$ integration in the cases of the transverse polar and planar phases.

$$\frac{1}{2\pi}\int_0^{2\pi} d\varphi' \hat{k}_i = \hat{q}_i \hat{\mathbf{q}}\cdot\hat{\mathbf{k}}, \tag{C8a}$$

$$\frac{1}{2\pi}\int_0^{2\pi} d\varphi' \hat{k}_i^2 = \hat{q}_i^2(\hat{\mathbf{q}}\cdot\hat{\mathbf{k}})^2 + \frac{1}{2}(1-\hat{q}_i^2)[1-(\hat{\mathbf{q}}\cdot\hat{\mathbf{k}})^2], \tag{C8b}$$

we obtain

$$\frac{1}{2\pi}\int_0^{2\pi} d\varphi' \frac{\ell_k}{\ell_q}\mathcal{T}^1_{00}(\mathbf{k},\mathbf{q}) \simeq \frac{1}{2\pi}\int_0^{2\pi} d\varphi' \frac{\ell_k}{\ell_q}\mathcal{T}^1_{t}(\mathbf{k},\mathbf{q}) \simeq \frac{2}{3} - \frac{1}{3}\frac{p^2}{\mu^2} + \frac{1}{24}\frac{p^4}{\mu^4}, \tag{C9}$$

where the approximation $k \simeq q \simeq \mu$ has been implemented via the replacements $\hat{\mathbf{q}}\cdot\hat{\mathbf{k}} \to 1 - p^2/(2\mu^2)$, $\hat{\mathbf{p}}\cdot\hat{\mathbf{k}} = -\hat{\mathbf{p}}\cdot\hat{\mathbf{q}} \to p/(2\mu)$. Now, we immediately compute $d = 9/2$, as listed in Table I.

2. Transverse planar phase

In this case, we find from Table II

$$\mathrm{Tr}[\mathcal{M}_{\mathbf{k}}\mathcal{M}^\dagger_{\mathbf{k}}\Lambda^+_{\mathbf{k}}] = 4(1+\hat{k}_3^2). \tag{C10}$$

Furthermore,

$$\mathcal{P}^+_{\mathbf{q},1} = \frac{1}{1+\hat{q}_3^2}[J_1^2(1-\hat{q}_1^2) + J_2^2(1-\hat{q}_2^2) - \{J_1, J_2\}\hat{q}_1\hat{q}_2 + J_3\hat{q}_3\gamma_0\gamma_5\boldsymbol{\gamma}\cdot\hat{\mathbf{q}}], \tag{C11}$$

where we have applied the identity

$$\gamma_{\perp,1}(\hat{\mathbf{q}})\gamma_{\perp,2}(\hat{\mathbf{q}}) - \hat{q}_1\hat{q}_2 = i\hat{q}_3\gamma_0\gamma_5\boldsymbol{\gamma}\cdot\hat{\mathbf{q}}. \tag{C12}$$

With the help of Eqs. (C10) and (C11) and the definitions (72) and (74), we compute the quantities $\mathcal{T}^s_{00}(\mathbf{k},\mathbf{q})$ and $\mathcal{T}^s_t(\mathbf{k},\mathbf{q})$. As in the polar phase, we find $\mathcal{T}^2_{00}(\mathbf{k},\mathbf{q}) = \mathcal{T}^2_t(\mathbf{k},\mathbf{q}) = 0$, hence $a_1 = 1$, $a_2 = 0$. For the gapped branch, $s = 1$, one obtains after taking the trace over color space,

$$\mathcal{T}^{\,1}_{\mu\nu}(\mathbf{k},\mathbf{q}) = -\frac{(\hat{q}_1^2 - \hat{q}_3^2 - 2)\mathcal{Q}^{11}_{\mu\nu} + (\hat{q}_2^2 - \hat{q}_3^2 - 2)\mathcal{Q}^{22}_{\mu\nu} + \hat{q}_1\hat{q}_2(\mathcal{Q}^{12}_{\mu\nu} + \mathcal{Q}^{21}_{\mu\nu}) + i\hat{q}_3(\mathcal{R}^{12}_{\mu\nu} - \mathcal{R}^{21}_{\mu\nu})}{6(1+\hat{k}_3^2)(1+\hat{q}_3^2)}, \tag{C13}$$

where the tensors $\mathcal{Q}$ and $\mathcal{R}$ are defined in Eqs. (C1). In order to perform the traces over Dirac space, one makes use of the identities (C2). We do not present the explicit results for $\mathcal{T}^1_{00}(\mathbf{k},\mathbf{q})$ and $\mathcal{T}^1_t(\mathbf{k},\mathbf{q})$ since they are too lengthy. In order to perform the angular integration, we proceed in a similar way as discussed above for the transverse polar phase. The difference is that in the planar phase the order parameter does not point into a special direction, but is located in the xy plane. Without loss of generality, we can assume $\hat{\mathbf{q}}$ to be also in the xy plane, $\hat{\mathbf{q}} = (\cos\varphi, \sin\varphi, 0)$ (cf. right diagram in Fig. 3). Note that this choice, in particular $\hat{q}_3 = 0$, immediately shows that the term proportional to γ_5 on the right-hand side of Eq. (C11) yields no contribution to the integral. Again, we rotate the frame such that the z' axis is parallel to $\hat{\mathbf{q}}$. This can be done with two successive rotations R_1 and $R_2(\varphi)$: First, we rotate the original frame by $\pi/2$ around the y axis,

$$R_1 = \begin{pmatrix} 0 & 0 & -1 \\ 0 & 1 & 0 \\ 1 & 0 & 0 \end{pmatrix}. \tag{C14}$$

Then, we rotate by φ around the new x' axis,

$$R_2(\varphi) = \begin{pmatrix} 1 & 0 & 0 \\ 0 & \cos\varphi & -\sin\varphi \\ 0 & \sin\varphi & \cos\varphi \end{pmatrix}. \tag{C15}$$

As above, in the new frame, $\hat{\mathbf{q}}' = (0, 0, 1)$ and $\hat{\mathbf{k}}' = (\sin\theta'\cos\varphi', \sin\theta'\sin\varphi', \cos\theta')$, and hence

$$\hat{\mathbf{k}} = R_1^{-1}R_2^{-1}(\varphi)\hat{\mathbf{k}}' = \begin{pmatrix} -\sin\theta'\sin\varphi'\sin\varphi + \cos\theta'\cos\varphi \\ \sin\theta'\sin\varphi'\cos\varphi + \cos\theta'\sin\varphi \\ -\sin\theta'\cos\varphi' \end{pmatrix}. \tag{C16}$$

With $\ell_k/\ell_q = (1 + \hat{k}_3^2)/(1 + \hat{q}_3^2)$ and the approximation $k \simeq q \simeq \mu$, we obtain

$$\frac{1}{2\pi}\int_0^{2\pi} d\varphi' \frac{\ell_k}{\ell_q}\mathcal{T}^1_{00}(\mathbf{k}, \mathbf{q}) \simeq \frac{1}{2\pi}\int_0^{2\pi} d\varphi' \frac{\ell_k}{\ell_q}\mathcal{T}^1_t(\mathbf{k}, \mathbf{q}) \simeq \frac{2}{3} - \frac{1}{3}\frac{p^2}{\mu^2} + \frac{1}{24}\frac{p^4}{\mu^4}. \tag{C17}$$

From these results we conclude $d = 9/2$.

3. Transverse A phase

In the transverse A phase, we have

$$\mathrm{Tr}[\mathcal{M}_{\mathbf{k}}\mathcal{M}^\dagger_{\mathbf{k}}\Lambda^+_{\mathbf{k}}] = 4(1 + \hat{k}_3^2). \tag{C18}$$

The projectors corresponding to the gapped excitations, $\mathcal{P}^+_{\mathbf{q},1/2}$ in Eqs. (B13), are

$$\mathcal{P}^+_{\mathbf{q},1/2} = \frac{1}{2}J_3^2\left\{1 \mp \frac{i}{|\hat{q}_3|}[\gamma_{\perp,1}(\hat{\mathbf{q}})\gamma_{\perp,2}(\hat{\mathbf{q}}) - \hat{q}_1\hat{q}_2]\right\} = \frac{1}{2}J_3^2\left(1 \pm \frac{\hat{q}_3}{|\hat{q}_3|}\gamma_0\gamma_5\boldsymbol{\gamma}\cdot\hat{\mathbf{q}}\right), \tag{C19}$$

where Eq. (C12) has been used. Inserting this projector and the respective quantities from Table III into Eq. (72), one obtains after taking the trace over color space,

$$\mathcal{T}^{1/2}_{\mu\nu}(\mathbf{k}, \mathbf{q}) = \frac{\mathrm{Tr}\{\gamma_\mu[\gamma_{\perp,1}(\hat{\mathbf{q}}) + i\gamma_{\perp,2}(\hat{\mathbf{q}})](1 \pm \frac{\hat{q}_3}{|\hat{q}_3|}\gamma_0\gamma_5\boldsymbol{\gamma}\cdot\hat{\mathbf{q}})\Lambda^-_{\mathbf{q}}\gamma_\nu[\gamma_{\perp,1}(\hat{\mathbf{k}}) - i\gamma_{\perp,2}(\hat{\mathbf{k}})]\Lambda^+_{\mathbf{k}}\}}{6(1 + \hat{k}_3^2)}, \tag{C20}$$

and $\mathcal{T}^3_{\mu\nu}(\mathbf{k}, \mathbf{q}) = 0$. Again, the results for the quantities $\mathcal{T}^{1,2}_{00}(\mathbf{k}, \mathbf{q})$ and $\mathcal{T}^{1,2}_t(\mathbf{k}, \mathbf{q})$, corresponding to the gapped branches, are complicated functions of $\hat{\mathbf{k}}$ and $\hat{\mathbf{q}}$, and we do not present their explicit forms.

As in the transverse planar phase, the order parameter for the transverse A phase points into a direction perpendicular to the z axis. However, in order to perform the angular integral over φ', we cannot make use of the same choice of the frame, because the assumption of $\hat{\mathbf{q}}$ being in the xy plane, i.e., $\hat{q}_3 = 0$, would lead to a division by zero according to Eq. (C20). Instead, we allow for the most general form, $\hat{\mathbf{q}} = (\sin\theta\cos\varphi, \sin\theta\sin\varphi, \cos\theta)$. In this case, the rotation of the original frame into the one with z' axis parallel to $\hat{\mathbf{q}}$ is given by

$$R(\theta, \varphi) = \begin{pmatrix} \cos\theta\cos\varphi & \cos\theta\sin\varphi & -\sin\theta \\ -\sin\varphi & \cos\varphi & 0 \\ \sin\theta\cos\varphi & \sin\theta\sin\varphi & \cos\theta \end{pmatrix}. \tag{C21}$$

Consequently, the $d\Omega_k$ integral has to be performed with

$$\hat{\mathbf{k}} = R^{-1}(\theta, \varphi)\hat{\mathbf{k}}' = \begin{pmatrix} \cos\varphi\cos\theta\sin\theta'\cos\varphi' - \sin\varphi\sin\theta'\sin\varphi' + \cos\varphi\sin\theta\cos\theta' \\ \sin\varphi\cos\theta\sin\theta'\cos\varphi' + \cos\varphi\sin\theta'\sin\varphi' + \sin\varphi\sin\theta\cos\theta' \\ -\sin\theta\sin\theta'\cos\varphi' + \cos\theta\cos\theta' \end{pmatrix}, \tag{C22}$$

where $\hat{\mathbf{k}}' = (\sin\theta'\cos\varphi', \sin\theta'\sin\varphi', \cos\theta')$ has been employed.

With $k \simeq q \simeq \mu$ one obtains

$$\frac{1}{2\pi}\int_0^{2\pi} d\varphi' \frac{\ell_k}{\ell_q}\mathcal{T}^{1/2}_{00}(\mathbf{k}, \mathbf{q}) \simeq \frac{1}{2\pi}\int_0^{2\pi} d\varphi' \frac{\ell_k}{\ell_q}\mathcal{T}^{1/2}_t(\mathbf{k}, \mathbf{q}) \simeq \frac{1}{2}\left(\frac{2}{3} - \frac{1}{3}\frac{p^2}{\mu^2} + \frac{1}{24}\frac{p^4}{\mu^4}\right)\left(1 \pm 2\frac{|\cos\theta|}{1 + \cos^2\theta}\right). \tag{C23}$$

The term $\pm 2|\cos\theta|/(1 + \cos^2\theta)$ on the right-hand side of this equation gives rise to a difference between the quantities $\mathcal{T}^1_{00,t}(\mathbf{k}, \mathbf{q})$ and $\mathcal{T}^2_{00,t}(\mathbf{k}, \mathbf{q})$. The origin of this difference is the term proportional to γ_5 on the right-hand side of Eq. (C19). As a consequence, one cannot choose the coefficients a_s such that they are constants cf. Eqs. (81). The transverse A phase is the only phase we consider, in which these coefficients depend on θ, the angle between $\hat{\mathbf{q}}$ and the

z axis. We find

$$a_1 = \frac{1}{2} + \frac{|\cos\theta|}{1+\cos^2\theta}, \qquad a_2 = \frac{1}{2} - \frac{|\cos\theta|}{1+\cos^2\theta}, \quad \text{(C24)}$$
$$a_3 = 0.$$

However, the constant d is identical to all other transverse phases, $d = 9/2$.

APPENDIX D: PROVING $\overline{d} = 6$ FOR ARBITRARY LONGITUDINAL GAPS

In this appendix, we prove $\overline{d} = 6$ for any order parameter (for any 3×3 matrix) Δ in the case of a longitudinal gap. The longitudinal case is particularly simple since the Dirac structure of the matrix $\mathcal{M}_{\mathbf{k}}$ is trivial.

Let us start with the matrix

$$\mathcal{M}_{\mathbf{k}} = \boldsymbol{v}_{\mathbf{k}} \cdot \boldsymbol{J}, \quad \text{(D1)}$$

where $\boldsymbol{v}_{\mathbf{k}} = (v_{\mathbf{k},1}, v_{\mathbf{k},2}, v_{\mathbf{k},3})$ is a 3-vector with

$$v_{\mathbf{k},i} \equiv \sum_{j=1}^{3} \Delta_{ij}\hat{k}_j, \qquad i = 1, 2, 3. \quad \text{(D2)}$$

Then,

$$(L^+_{\mathbf{k}})_{ij} = v^2_{\mathbf{k}}\delta_{ij} - v^*_{\mathbf{k},j}v_{\mathbf{k},i}, \quad \text{(D3)}$$

where $v^2_{\mathbf{k}} \equiv \boldsymbol{v}^*_{\mathbf{k}} \cdot \boldsymbol{v}_{\mathbf{k}}$. Now, with $(L^+_{\mathbf{k}})^2 = v^2_{\mathbf{k}} L^+_{\mathbf{k}}$ and $\mathrm{Tr}L^+_{\mathbf{k}} = 8v^2_{\mathbf{k}}$ the eigenvalues of $L^+_{\mathbf{k}}$ are easily found making use of the method shown in Appendix B. One obtains

$$\lambda_{k,1} = v^2_{\mathbf{k}} \quad \text{(8-fold)}, \qquad \lambda_{k,2} = 0 \quad \text{(4-fold)}. \quad \text{(D4)}$$

Consequently, the fact that there is one gapped branch with degeneracy 8 and one ungapped branch with degeneracy 4 is completely general, i.e., it is true for any order parameter in the longitudinal case. The corresponding projectors are given by

$$(\mathcal{P}^+_{\mathbf{k},1})_{ij} = \delta_{ij} - \frac{v^*_{\mathbf{k},j}v_{\mathbf{k},i}}{v^2_{\mathbf{k}}}, \qquad (\mathcal{P}^+_{\mathbf{k},2})_{ij} = \frac{v^*_{\mathbf{k},j}v_{\mathbf{k},i}}{v^2_{\mathbf{k}}}. \quad \text{(D5)}$$

This leads to

$$\mathcal{T}^1_{00}(\mathbf{k},\mathbf{q}) = \frac{1}{3}\frac{\boldsymbol{v}_{\mathbf{q}} \cdot \boldsymbol{v}^*_{\mathbf{k}}}{v^2_{\mathbf{k}}}(1 + \hat{\mathbf{q}} \cdot \hat{\mathbf{k}}),$$
$$\mathcal{T}^1_t(\mathbf{k},\mathbf{q}) = \frac{2}{3}\frac{\boldsymbol{v}_{\mathbf{q}} \cdot \boldsymbol{v}^*_{\mathbf{k}}}{v^2_{\mathbf{k}}}(1 - \hat{\mathbf{p}} \cdot \hat{\mathbf{q}}\,\hat{\mathbf{p}} \cdot \hat{\mathbf{k}}), \quad \text{(D6)}$$

and $\mathcal{T}^2_{00}(\mathbf{k},\mathbf{q}) = \mathcal{T}^2_t(\mathbf{k},\mathbf{q}) = 0$, hence $a_1 = 1$, $a_2 = 0$. The angular integration is done as explained for the transverse A phase in the previous appendix, i.e., the rotation given by Eq. (C21) and the respective expressions for the vectors $\hat{\mathbf{k}}$ and $\hat{\mathbf{q}}$ are used.

With $\ell_k/\ell_q = \lambda_{k,1}/\lambda_{q,1} = v^2_{\mathbf{k}}/v^2_{\mathbf{q}}$ we obtain

$$\frac{1}{2\pi}\int_0^{2\pi} d\varphi' \frac{\ell_k}{\ell_q}\frac{\boldsymbol{v}_{\mathbf{q}} \cdot \boldsymbol{v}^*_{\mathbf{k}}}{v^2_{\mathbf{k}}} = \hat{\mathbf{q}} \cdot \hat{\mathbf{k}}, \quad \text{(D7)}$$

where Eq. (C8a) has been used. Therefore, we find with $k \simeq q \simeq \mu$,

$$\frac{1}{2\pi}\int_0^{2\pi} d\varphi' \frac{\ell_k}{\ell_q}\mathcal{T}^1_{00}(\mathbf{k},\mathbf{q}) \simeq \frac{1}{2\pi}\int_0^{2\pi} d\varphi' \frac{\ell_k}{\ell_q}\mathcal{T}^1_t(\mathbf{k},\mathbf{q})$$
$$\simeq \frac{2}{3} - \frac{1}{2}\frac{p^2}{\mu^2} + \frac{1}{12}\frac{p^4}{\mu^4}, \quad \text{(D8)}$$

which, making use of the definitions (81) and (84), proves the universal result $d = 6$ for longitudinal gaps. Since $d = \overline{d}$ when d is constant cf. definition (94), we conclude $\overline{d} = 6$.

[1] J. Bardeen, L. N. Cooper, and J. R. Schrieffer, Phys. Rev. **108**, 1175 (1957).
[2] D. Bailin and A. Love, Phys. Rep. **107**, 325 (1984).
[3] M. Alford, K. Rajagopal, and F. Wilczek, Nucl. Phys. **B537**, 443 (1999).
[4] M. G. Alford, J. A. Bowers, and K. Rajagopal, Phys. Rev. D **63**, 074016 (2001).
[5] A. I. Larkin and Y. N. Ovchinnikov, Zh. Eksp. Teor. Fiz. **47**, 1136 (1964); P. Fulde and R. A. Ferrell, Phys. Rev. **135**, A550 (1964).
[6] I. Shovkovy and M. Huang, Phys. Lett. B **564**, 205 (2003); Nucl. Phys. **A729**, 835 (2003).
[7] M. Alford, C. Kouvaris, and K. Rajagopal, Phys. Rev. Lett. **92**, 222001 (2004); S. B. Rüster, I. A. Shovkovy, and D. H. Rischke, Nucl. Phys. **A743**, 127 (2004); K. Fukushima, C. Kouvaris, and K. Rajagopal, Phys. Rev. D **71**, 034002 (2005).
[8] P. F. Bedaque and T. Schäfer, Nucl. Phys. **A697**, 802 (2002); A. Kryjevski, D. B. Kaplan, and T. Schäfer, Phys. Rev. D **71**, 034004 (2005); A. Kryjevski and D. Yamada, Phys. Rev. D **71**, 014011 (2005).
[9] H. Müther and A. Sedrakian, Phys. Rev. D **67**, 085024 (2003).
[10] M. Iwasaki and T. Iwado, Phys. Lett. B **350**, 163 (1995); R. D. Pisarski and D. H. Rischke, Phys. Rev. D **61**, 051501 (2000); M. G. Alford, J. A. Bowers, J. M. Cheyne, and G. A. Cowan, Phys. Rev. D **67**, 054018 (2003); M. Buballa, J. Hošek, and M. Oertel, Phys. Rev. Lett. **90**, 182002 (2003).
[11] R. D. Pisarski and D. H. Rischke, Phys. Rev. D **61**, 074017 (2000).
[12] T. Schäfer, Phys. Rev. D **62**, 094007 (2000).
[13] A. J. Leggett, Rev. Mod. Phys. **47**, 331 (1975).
[14] D. Vollhardt and P. Wölfle, *The Superfluid Phases of*

Helium 3 (Taylor & Francis, London, 1990).
[15] T. Schäfer and F. Wilczek, Phys. Rev. D **60**, 114003 (1999); D. K. Hong, V. A. Miransky, I. A. Shovkovy, and L. C. R. Wijewardhana, Phys. Rev. D **61**, 056001 (2000); **62**, 059903(E) (2000).
[16] D. T. Son, Phys. Rev. D **59**, 094019 (1999).
[17] W. E. Brown, J. T. Liu, and H.-C. Ren, Phys. Rev. D **61**, 114012 (2000); **62**, 054013 (2000); **62**, 054016 (2000).
[18] Q. Wang and D. H. Rischke, Phys. Rev. D **65**, 054005 (2002).
[19] A. Schmitt, Q. Wang, and D. H. Rischke, Phys. Rev. D **66**, 114010 (2002).
[20] L. Michel, Rev. Mod. Phys. **52**, 617 (1980).
[21] A. Schmitt, Q. Wang, and D. H. Rischke, Phys. Rev. Lett. **91**, 242301 (2003).
[22] A. Schmitt, Q. Wang, and D. H. Rischke, Phys. Rev. D **69**, 094017 (2004).
[23] D. H. Rischke, Phys. Rev. D **62**, 054017 (2000).
[24] J. M. Cornwall, R. Jackiw, and E. Tomboulis, Phys. Rev. D **10**, 2428 (1974).
[25] D. H. Rischke, Prog. Part. Nucl. Phys. **52**, 197 (2004).
[26] H. Abuki, Prog. Theor. Phys. **110**, 937 (2003).
[27] S. B. Rüster and D. H. Rischke, Phys. Rev. D **69**, 045011 (2004).
[28] C. Manuel, Phys. Rev. D **62**, 114008 (2000).
[29] A. Schmitt, Ph.D. dissertation (nucl-th/0405076).
[30] D. H. Rischke, Phys. Rev. D **64**, 094003 (2001).
[31] V. A. Miransky, I. A. Shovkovy, and L. C. R. Wijewardhana, Phys. Lett. B **468**, 270 (1999); I. A. Shovkovy and P. J. Ellis, Phys. Rev. C **66**, 015802 (2002).
[32] A. Gerhold and A. Rebhan, Phys. Rev. D **68**, 011502 (2003); D. D. Dietrich and D. H. Rischke, Prog. Part. Nucl. Phys. **53**, 305 (2004).
[33] C. C. Tsuei and J. R. Kirtley, Rev. Mod. Phys. **72**, 969 (2000); K. Izawa, K. Kamata, Y. Nakajima, Y. Matsuda, T. Watanabe, M. Nohara, H. Takagi, P. Thalmeier, and K. Maki, Phys. Rev. Lett. **89**, 137006 (2002).
[34] M. Alford, P. Jotwani, C. Kouvaris, J. Kundu, and K. Rajagopal, astro-ph/0411560.
[35] H. Grigorian, D. Blaschke, and D. Voskresensky, astro-ph/0411619 [Phys. Rev. C (to be published)].